Comprehensive numerical and analytical study of two holes doped into the two-dimensional *t-J* model

A. L. Chernyshev*
Department of Physics, Queen's University, Kingston, Ontario, Canada K7L 3N6

P. W. Leung
Physics Department, Hong Kong University of Science and Technology, Clear Water Bay, Hong Kong

R. J. Gooding
Department of Physics, Queen's University, Kingston, Ontario, Canada K7L 3N6
(Received 20 May 1998)

We report on a detailed examination of numerical results and analytical calculations devoted to a study of two holes doped into a two-dimensional, square lattice described by the *t-J* model. Our exact diagonalization numerical results represent the first solution of the exact ground state of two holes in a 32-site lattice. Using this wave function, we have calculated several important correlation functions, notably the electron momentum distribution function and the hole-hole spatial correlation function. Further, by studying similar quantities on smaller lattices, we have managed to perform a finite-size scaling analysis. We have augmented this work by endeavouring to compare these results to the predictions of analytical work for two holes moving in an infinite lattice. This analysis relies on the canonical transformation approach formulated recently for the *t-J* model. From this comparison we find excellent correspondence between our numerical data and our analytical calculations. We believe that this agreement is an important step helping to justify the quasiparticle Hamiltonian, and, in particular, the quasiparticle interactions that result from the canonical transformation approach. Also, the analytical work allows us to critique the finite-size scaling ansatzes used in our analysis of the numerical data. One important feature that we can infer from this successful comparison involves the role of higher harmonics in the two-particle, *d*-wave symmetry bound state—the conventional $[\cos(k_x)-\cos(k_y)]$ term is only one of many important contributions to the *d*-wave symmetry pair wave function. [S0163-1829(98)04044-2]

I. INTRODUCTION

The behavior of mobile holes in an antiferromagnetic (AF) spin background has been a subject of intensive study, in part because of its possible connection to high-temperature superconductivity. The ubiquitous structural components of such materials are the CuO_2 planes, and a simplified description of carriers in these planes is the theoretical focus of this paper. We consider the so-called *t-J* model,[1,2] for which the holes correspond to the Zhang-Rice singlets,[3] mobile vacancies created by doping a single CuO_2 plane. A microscopic representation of this model is

$$\mathcal{H}_{t-J}=-t\sum_{\langle ij\rangle\sigma}(\tilde{c}^{\dagger}_{i\sigma}\tilde{c}_{j\sigma}+\text{H.c.})+J\sum_{\langle ij\rangle}(\mathbf{S}_i\cdot\mathbf{S}_j-\tfrac{1}{4}n_in_j), \tag{1}$$

where $\langle ij\rangle$ denotes nearest-neighbor sites, and $\tilde{c}^{\dagger}_{i\sigma}$, $\tilde{c}_{i\sigma}$ are the constrained operators, $\tilde{c}_{i\sigma}=c_{i\sigma}(1-c^{\dagger}_{i,-\sigma}c_{i,-\sigma})$. The ratio of the AF exchange constant to the hopping amplitude is believed to be $J/t\sim 0.3$.

Aided by recent angle-resolved photoemission experiments,[4] followed by extensive comparisons between theory and experiment,[5] it is now recognized that this simple, near-neighbor hopping Hamiltonian on its own is insufficient to fully represent the true single-hole state of the real CuO_2 plane. Hoppings between more distant neighbors are required,[5–7] as are more complicated three-site spin-dependent hoppings. Possibly, the full three-band microscopic Hamiltonian is necessary.[8]

Despite the potential inadequacy of this Hamiltonian to represent completely the CuO_2 planes, it is still the simplest model that captures the important antiferromagnetic correlations of a weakly doped antiferromagnet.[9] Thus, it is crucial that the properties of this model when doped are elucidated.

The Hamiltonian in Eq. (1) has been investigated intensively by different analytical and numerical methods, and we believe that a consistent picture is emerging from these studies. For example, results obtained from exact diagonalization numerical work on small clusters with periodic boundary conditions, such as the energy spectrum and quasiparticle residue, have been found to be in the excellent agreement with the behavior predicted by a well-studied analytical theory.[10] However, a large amount of the numerical data for the correlation functions at present are not well understood and require further investigation. Such work could help to *justify the correct quasiparticle model for the system of strongly interacting holes and spins at low energies*. It is in this manner that we unite our analytical and numerical work in this paper.

Our analytical approach follows from a phenomenology of a common and apparently successful theory of a single hole moving in an AF aligned background, and involves the so-called spin polaron.[11–14] According to the spin-polaron idea, the hole in its movement disturbs the magnetic background that one can formally describe as the strong coupling

of the hole and spin degrees of freedom. This makes this problem similar to the well-known strong-coupling electron-phonon one. However, in spite of the qualitative similarity of these two polarons, there is an essential difference between them. If the phonon polaron can be considered as an almost static object of the shifted ions with the electron in the center, the spin polaron is the ''spin bag'' with the *moving* hole inside. One of the statements of the present paper is that this feature of the spin polaron is responsible for the absence of the direct similarity between the answers that theory provides for *quasiparticles* and the numerically obtained data for *bare* holes. A similar conclusion, using a different analytical approach and numerical results for smaller clusters, was reached by Eder and co-workers.[15–17] Later, similar remarks were made by Riera and Dagotto.[18]

In this paper we combine analytical and exact diagonalization (ED) numerical results of the one- and two-hole problem to provide a comprehensive study of these important systems. Computationally we have managed, for the first time, to determine the two-hole ground state for two holes doped into the 32-site, square cluster used by two of us in a previously published numerical work.[10] We find that the lowest-energy state is a $\mathbf{P}=0$ bound state with $d_{x^2-y^2}$ symmetry. We have characterized the ground state by evaluating a number of important expectation values, notably, the electron momentum distribution function (EMDF), and the spatial pair-correlation function.

We have found that an effective quasiparticle Hamiltonian, originally proposed by Belinicher, one of us, and Shubin,[19] may be used to calculate the same expectation values that were obtained numerically via ED. Further, these quantities are remarkably similar to those obtained via ED. This gives strong support to the appropriateness of this quasiparticle Hamiltonian.

Previous analytical work on the low-energy physics of the two-hole system generally describes it in terms of moderately interacting spin polarons. This analytical work shows that the dominant effective interactions between spin polarons come from the short-range nearest-neighbor static attraction and spin-wave exchange, the latter leading to a long-range dipolar interaction. These interactions are attractive for *d*-wave states and strongly repulsive for *s*-wave states. The purpose of this paper is to use the ED results to provide support for this description of the internal structure of the quasiparticles, and indirectly for the above-mentioned description[19] of their interactions.

We will first describe the present status of the *t*-*J* model studies in Sec. II. Section III discusses in detail the numerical data available for the ground-state correlation functions. Then, Sec. IV summarizes briefly the analytical results of relevant previous work and displays the details of the present calculations. Section V focuses on the comparison of the analytical and numerical results, and in Sec. VI we present our conclusions.

II. PREVIOUS *T*-*J* MODEL STUDIES

A. Analytical results

Theoretical studies of the *t*-*J* model have resulted in a clear understanding of the nature of the low-energy excitations for the system near half-filling. The charge carrier created by a hole introduced in an AF background is described as a spin polaron, viz. as a quasiparticle consisting of a hole and a cloud of spin excitations. The AF spin-polaron concept was put forward in earlier works of Bulaevskii, Nagaev, and Khomskii[11] and Brinkman and Rice,[20] and then developed in a number of more recent papers[12–14,21–28] using different techniques.

The main conclusion of these papers was that the spin polaron in an AF background is a well-defined quasiparticle with a nonzero residue and a specific dispersion law. The dressing of the hole leads to the narrow quasiparticle band with a bandwidth $\sim 2J$ for realistic J/t, band minima at $\mathbf{k}=\pm(\pi/2,\pm\pi/2)$, and a heavy effective mass along the magnetic Brillouin zone (MBZ) boundary. Most of these features of the spin polaron were found to be robust under generalizations of the *t*-*J* model,[29] including further neighbor and three-site hoppings, and for a wide range of J/t ratio.

The single-hole problem has been treated analytically in detail.[11–14,20,22–27,30] Grouping these efforts, two approaches in treating this problem were used: (i) the self-consistent Born approximation (SCBA) (e.g., see Refs. 13, 14, and 22), and (ii) the so-called ''string'' approach (e.g., see Refs. 11, 20, 23, and 25–27). Recently, a relationship between these two has been established.[31] We briefly review these methods with an eye to understanding how well they might be able to describe the two-hole or multihole problem.

The SCBA method utilizes a property of the hole-magnon interaction, namely, the absence of the lowest-order correction to the Born approximation series for the single-particle Green's function.[13,14,22] The attractive feature of the SCBA approach is that the essentially exact single-hole spectral functions can be evaluated quite easily using simple numerical calculations. Recently, the detailed structure of the single-hole ground state and behavior of different correlators has been studied using SCBA.[32] Unfortunately, already in two- or many-hole problems much more involved numerical and analytical efforts are required.[33]

The string approach is based on the idea that in an AF background a hole will be confined by an effective potential created by overturned spins (strings). Formally, the real-space variational ansatz for the polaron's wave function with the strings of different length is considered to reproduce this tendency. In spite of the considerable success of the string approach for the single-hole problem,[25] there are some problems that make the use of it as a candidate for a quasiparticle theory for the *t*-*J* model questionable. First of all, the string method uses the real-space approach, which does not treat properly the long-range dynamics of the system. The next problem is that the method starts from the Ising background and includes fluctuations on a perturbative basis, whereas the fluctuations are strong in two dimensions and must be ''built in'' to the real ground state of the spin system. The third problem concerns the necessity of the normal anticommutation relations of the quasiparticle operators. If a hole is a fermion a unitary transformation, which diagonalizes the Hamiltonian and dresses the hole by the spin excitations, would not change its statistics. Within the variational string and other approaches, one works with the wave functions and usually identifies the wave function of the quasiparticle with the *operator* of the quasiparticle. This leads to the absence of the commutation relations for these operators and to

troubles with the proper normalization and orthogonality of the states already for the two-hole problem.[18,34] Because of that one cannot correctly derive the effective polaron-polaron interaction term using a single-hole wave function.

These difficulties notwithstanding, several attempts to address the two-hole ground state have been made. Work based on the string approach has led to some qualitative understanding of the problem.[17,23,35]

The investigation of the interactions between quasiparticles in the t-J model is a subject of prime interest in the context of the magnetic pairing mechanism. However, studies of this problem show much less convergence than the single-hole problem. Other work involves the formulation of an effective model for spin polarons propagating in the AF background.[30,36–39] From the random phase approximation (RPA) treatment of the Hubbard model in the strong-coupling limit, the model of ''spin bags'' interacting via longitudinal magnetization fluctuations has been proposed.[37] A phenomenological model for the vacancies coupled by the long-range dipolar twist of the spin background has been also worked out[30,40] using a semiclassical hydrodynamic approach. Inspired by the numerical evidence of the hole-hole d-wave bound state and the Van Hove singularity in the single-hole spectrum, taking the simplest phenomenological form of the interaction, an AF Van Hove model has been put forward.[39] Using an ansatz for the quasiparticle wave function,[27] the ''contact'' hole-hole and the residual hole-magnon interactions have been obtained,[41,42] and then the effective Hamiltonian for the polarons and long-range spin waves has been presented.[36]

Even though most of these theories were formulated on a phenomenological and semiphenomenological basis, they provided two key interactions leading to pairing in the t-J model. One of them is the effective hole-hole static attraction due to minimization of the number of broken bonds found from placing two holes at nearest-neighbor sites (sometimes referred to as the ''sharing common link effect''). The other is due to spin-wave exchange, and leads to a dipolar-type interaction between holes.[30,36,43]

Quite recently, a new approach to the derivation of a quasiparticle model from the t-J model has been developed.[19] It used a generalization of the canonical transformation (CT) approach of the Lang-Firsov type. An effective Hamiltonian for the spin polarons includes in itself both types of the hole-hole interactions mentioned above in a natural way. Some details of this approach are presented in Sec. IV. In Ref. 19 results for the single-hole properties have been compared with those of the SCBA calculations and an impressive agreement has been found. This is supported further by the idea that the ''canonically transformed'' quasiparticles are close to exact t-J model ones. Even though the CT approach is less controlled than the SCBA one, it solves naturally all the problems mentioned above and allows one to derive the quasiparticle Hamiltonian for interacting spin polarons from the original t-J model. Thus, in this paper we compare the predictions obtained from this Hamiltonian to our numerics, and in this way we critique the description of the interactions between quasiparticles that follows from the CT approach.

B. Numerical studies

ED studies of the t-J model doped away from half-filling on small clusters with periodic boundary conditions are an important source of unbiased information on the low-energy physics of this system. One- and two-hole ground states have been investigated in great detail on the 16- (4×4),[44–52] 18- $(\sqrt{18}\times\sqrt{18})$, 20- $(\sqrt{20}\times\sqrt{20})$,[53–62] and 26-site $(\sqrt{26}\times\sqrt{26})$ (Refs. 63–69) clusters. Although some of these results converge, at least partially, these clusters suffer from various finite-size problems. The 20- and 26-site clusters do not have the full rotational symmetry of the square lattice. Therefore, they do not possess important reciprocal lattice points along the high-symmetry directions in the first Brillouin zone. For example, the important reciprocal lattice point $(\pi/2,\pi/2)$ does not exist in the first Brillouin zone of the 18-, 20-, and 26-site clusters. This causes the ground-state momenta of the one-hole state to be different from the predicted $\pm(\pi/2,\pm\pi/2)$ points. Although the 16-site cluster has the $(\pi/2,\pi/2)$ point, it has an additional symmetry that causes an accidental degeneracy of the levels at $(\pi/2,\pi/2)$ and $(\pi,0)$ for one hole, and between (0,0) and $(\pi,0)$ for the two-hole problem.[52] Attempts to remedy the missing $(\pi/2,\pi/2)$ point have been made by using the nonsquare 16-site $(\sqrt{8}\times\sqrt{32})$ (Ref. 70) and 24-site $(\sqrt{18}\times\sqrt{32})$ (Ref. 71) clusters.

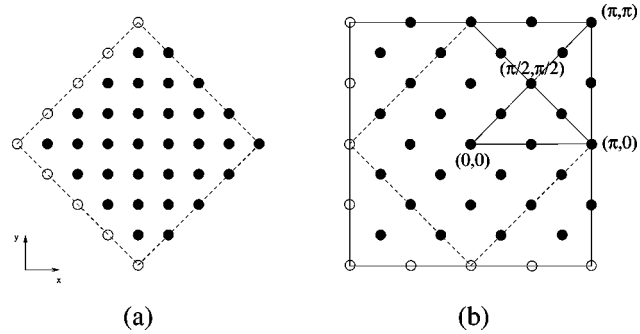

FIG. 1. The 32-site cluster in (a) direct and (b) reciprocal space. Empty circles are included to mimic the periodic boundary conditions used in our studies. The solid lines in (b) show the important directions in **k** space displaying the high symmetry of the cluster. The dashed line in (b) borders the first magnetic Brillouin zone.

Previous results on the single-hole problem show that the quasiparticle peak at the bottom of the spectral function can be expected to survive in the thermodynamic limit.[10,45,48,64] The corresponding quasiparticle band is narrow (of the order of $2J$ in the ''physical'' region $J/t<1$) and the band minima are shifted to the antiferromagnetic Brillouin zone (ABZ) boundary. However, due to the previously mentioned deficiencies of the 16-, 18-, 20-, and 26-site clusters, none of them can actually show that the quasiparticle minima are at the $\pm(\pi/2,\pm\pi/2)$ points; these wave vectors are those predicted by numerous theoretical studies.[12,21,23,30]

The smallest cluster that has the full rotational symmetry of the square lattice contains the $(\pi/2,\pi/2)$ point, and is free from the spurious degeneracies mentioned above, is the 32-site cluster $(\sqrt{32}\times\sqrt{32})$—see Fig. 1. Also, it is the largest such system that can be solved using modern computers. These calculations involve finding the lowest-energy states of matrices with dimensions of up to 300 million.

Recently, some results for the single-hole problem have been published for this cluster by two of us.[10] These numerics showed that the effective mass around the minima is anisotropic, and that the quasiparticle residue is rather small for

realistic J/t, both in excellent agreement with analytical predictions. Further, the full dispersion relation predicted by analytical work based on the SCBA (Refs. 13, 14, and 22) is found to be in excellent agreement with ED numerics on this cluster.[10]

ED results for two holes on finite clusters consistently show that they are coupled in a bound state with $d_{x^2-y^2}$ symmetry in a wide range of J/t,[44,46,47,49,50,52,55,56,61,67–69,72] in agreement with earlier ED data for the 16-site Hubbard model,[73,74] the Green's function Monte Carlo studies on 8×8 cluster,[75] and some theories.[17,19,36–39,76] Low-lying states with other symmetries, as well as $\mathbf{k}\neq(0,0)$ states, have also been studied.[49,61] Attempts have been made to extrapolate the binding energy to the thermodynamic limit and thus to estimate the critical value of J/t for the formation of a bound state.[67,69] Also, some knowledge concerning the internal structure of the bound state is known.[68,75] Lastly, the electron momentum distribution function has been investigated in order to search for Fermi-like discontinuities. Drastic differences between the single-hole and two-hole cases have been noted.[51,57,58] Finite-size and J/t scalings of this quantity have also been studied.[58,59,62]

Nevertheless, the above-mentioned results are of limited usefulness simply because of the systematic error introduced by the lower symmetry of the clusters with 16, 18, 20, and 26 sites. Clearly, the 32-site cluster would augment such studies. Further, with the collection of all such clusters, and some analytical guidance regarding the correct scaling laws, information on the thermodynamic limit, viz. a density of zero [two holes in an infinite two-dimensional (2D) square lattice], would be accessible.

Section III will summarize the results of the ED studies of the single- and two-hole problems that we have obtained on the 32-site cluster. Some of the single-hole results have been published previously,[10] and we only mention those results that are crucial to our scaling analyses. A brief summary of a portion of the two-hole comparison to the CT Hamiltonian was presented in Ref. 77.

III. NUMERICAL WORK

Most of the results presented in this section are obtained by ED on the 32-site cluster with periodic boundary conditions for the realistic value $J/t=0.3$. Results at different J/t, as well as on smaller clusters published previously,[51,67] are also used in the discussion of the finite-size scaling (FSS), bound-state energies, and correlation functions.

To look for evidence of hole binding in the low-energy states, we calculate the two–hole binding energy $E_b\equiv E_2-2E_1+E_0$, where E_1 and E_0 are the ground-state energies with one and no hole, respectively, and E_2 is the energy of the two-hole state. Further, two expectation values that we are interested in are defined as follows: (i) The electron momentum distribution function (EMDF) is given by $\langle n_{\mathbf{k}\sigma}\rangle \equiv\langle \tilde{c}^{\dagger}_{\mathbf{k}\sigma}\tilde{c}_{\mathbf{k}\sigma}\rangle$, where $\tilde{c}^{\dagger}_{\mathbf{k}\sigma}$, $\tilde{c}_{\mathbf{k}\sigma}$ are the Fourier transform of the constrained operators. (ii) The spatial distribution of holes in the bound state is characterized by the pair-correlation function defined as

$$C(r)=\frac{1}{N_hN_E(r)}\sum_{i,j}\langle(1-n_i)(1-n_j)\delta_{|i-j|,r}\rangle, \qquad (2)$$

where N_h is the number of holes, and $N_E(r)$ is the number of equivalent sites at a distance r from any given site.

Before presenting the FSS of the EMDF, we discuss what kind of finite-size behavior one can expect. The EMDF is expected to show how hole doping changes the uniform value of $\langle n_{\mathbf{k}\sigma}\rangle=\frac{1}{2}$ obtained in the half-filled case. In a system of free particles, a hole with a certain momentum will manifest itself as the complete suppression of $\langle n_{\mathbf{k}\sigma}\rangle$ to zero at this momentum. In systems with interaction the physics of which can be described in terms of the quasiparticles, this suppression will be proportional to the quasiparticle residue $Z_{\mathbf{k}}$, and is almost independent of the cluster size; the rest of the hole weight will be distributed among the other available $\mathbf{k}$ points. Consequently, the more $\mathbf{k}$ points a system possesses the less hole weight each $\mathbf{k}$ point will carry. Therefore, in the single-hole problem we anticipate that $\langle n_{\mathbf{k}\sigma}\rangle$ for the ground-state momentum $\mathbf{P}$ to be suppressed by a constant proportional to $Z_{\mathbf{P}}$. Further, we expect that the deviation from the half-filled value,

$$\langle \delta n_{\mathbf{k}\sigma}\rangle=\langle n_{\mathbf{k}\sigma}\rangle-\tfrac{1}{2}, \qquad (3)$$

will scale as $1/N$ at all other points until (roughly) the physics of the system does not change with the cluster size, i.e., when size of the quasiparticle is smaller than the cluster size.

The same argument should apply to the bound states of the two-hole problem, where we predict $\langle \delta n_{\mathbf{k}\sigma}\rangle$ to scale as $1/N$ at all $\mathbf{k}$ points.

A. Single-hole case

We wish to provide a FSS analysis of certain quantities for the two-hole ground state. To this end, we present new results for the one-hole problem that will facilitate such work.

Figure 2 shows the EMDF of the single-hole ground state on the 32-site cluster at $J/t=0.3$, which has total spin $S^z_{tot}=+\frac{1}{2}$ and momentum $\mathbf{P}=(\pi/2,\pi/2)$. Due to the nonzero momentum of this state, the only symmetry its EMDF has is a reflection about the ''main diagonal'' [$(-\pi,-\pi)\leftrightarrow(\pi,\pi)$ line].

Several features of the EMDF are worth noticing. First, $\langle n_{\mathbf{k}\downarrow}\rangle$ has a ''dip'' at the GS momentum $\mathbf{P}$. Earlier studies of the J/t dependence of the intensity of this dip have left no doubt about its direct relation to the quasiparticle weight $Z_{\mathbf{P}}$.[58] Second, the EMDF deviates significantly from its half-filled value for both spin directions across the entire Brillouin zone. This background has a maximum at (0,0) and a minimum at (π,π), which is a by-product of minimizing the kinetic energy of the system[16]. Although this ''dome'' shape resembles the ''large Fermi surface'' in a system of free electrons, it has different physics behind it. The discussion of this behavior will be given in Sec. IV. One observes that this dome structure in $\langle n_{\mathbf{k}\uparrow}\rangle$ is shifted upwards from its half-filled value, and that in $\langle n_{\mathbf{k}\downarrow}\rangle$ it is shifted downwards ($\langle n_{(0,0)\uparrow}\rangle-\langle n_{(0,0)\downarrow}\rangle\simeq 0.03$). The difference between the maximum and minimum,

$$\Delta n_{\sigma}=\langle n_{(0,0)\sigma}\rangle-\langle n_{(\pi,\pi)\sigma}\rangle, \qquad (4)$$

is slightly larger for $\sigma=\uparrow$ than for $\downarrow$ [$\Delta n_{\uparrow(\downarrow)}\simeq 0.07(0.06)$ at $J/t=0.3$]. Also $\Delta n_{\downarrow}$ has a stronger J/t dependence. Finally,

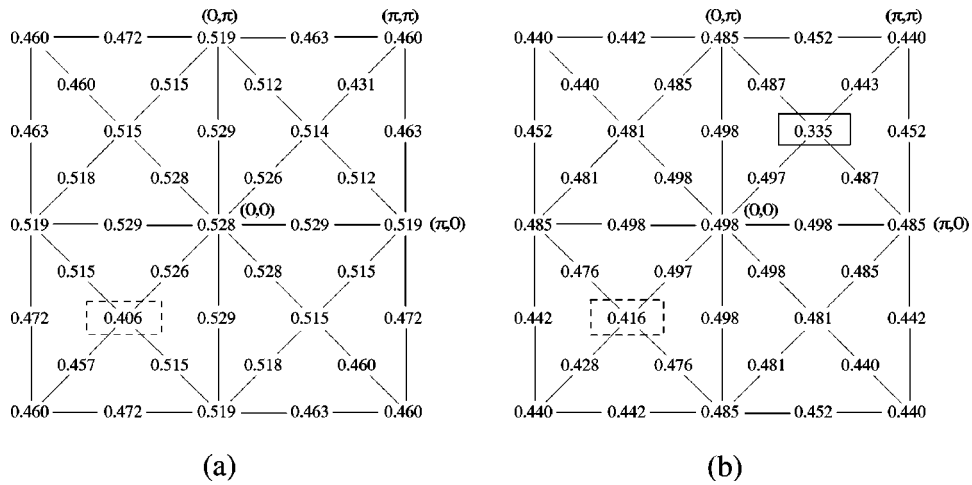

FIG. 2. The EMDF for the single-hole ground state having momentum $\mathbf{P}=(\pi/2,\pi/2)$ and $S^z_{tot}=+1/2$ at $J/t=0.3$. The numbers are the electron filling factors (a) $\langle n_{\mathbf{k}\uparrow}\rangle$, (b) $\langle n_{\mathbf{k}\downarrow}\rangle$ at the corresponding $\mathbf{k}$ points. Antidips at $(-\pi/2,-\pi/2)$ described in the text are denoted by the dashed boxes, and the dip in (b) at the ground-state momentum is highlighted by the solid box.

the EMDF's of both $\sigma=\uparrow,\downarrow$ have ''antidips'' at $(-\pi/2,-\pi/2)$. They were observed earlier but no successful explanation has been presented. The fact that the antidips are always at $\mathbf{P}-\mathbf{Q}_{AF}$ supports the idea that their physics is somehow related to the long-range AF fluctuations in the system.[58] Subtraction of the ''normal'' background from $\langle n_{(-\pi/2,-\pi/2)\sigma}\rangle$ shows that the depth of the antidip,

$$\Delta n_{anti,\sigma}=\langle n_{(-\pi/2,-\pi/2)\sigma}\rangle-\langle n_{(\pi/2,-\pi/2)\sigma}\rangle, \tag{5}$$

is larger for $\uparrow$ $[\Delta n_{anti,\uparrow(\downarrow)}\simeq 0.11(0.08)$ at $J/t=0.3]$, and $\Delta n_{anti,\downarrow}$ has stronger J/t dependence.

In Figs. 3 and 4 we plot $\langle \delta n_{\sigma\mathbf{k}}\rangle$ vs the ''inverse volume'' of the system, $1/N$, at $J/t=0.3$ for all $\mathbf{k}$ points (except $\mathbf{P}$ and $\mathbf{P}-\mathbf{Q}_{AF}$) available on more than one cluster. One finds results consistent with a $1/N$ scaling at all of these points, in agreement with our expectations. Figure 5 shows the same plot for the EMDF at the ground-state momentum. Extrapolation to the thermodynamic limit shows that the dip, which we expect to be $Z_{\mathbf{P}}/2$ (the factor one-half is from the proper normalization of the wave function), is about 0.14, or $Z_{\mathbf{P}}\simeq 0.28$. This agrees well with SCBA result, $Z_{\mathbf{P}}^{SCBA}=0.271$.[13] There is no simple scaling for the antidips of $|\langle \delta n_{\mathbf{P}-\mathbf{Q}\sigma}\rangle|$ because of the long-range physics involved. According to the discussion in Sec. IV they are combinations of terms with different scaling behaviors.

B. Two-hole case

The only zero total momentum bound state that we have found in the zero magnetization channel is a singlet and it has $d_{x^2-y^2}$ symmetry. Figure 6(a) shows the J/t dependence of the binding energy E_b on the 16-, 26-, and 32-site clusters. One can see that the absolute value of the binding energy gets smaller as the size of the cluster grows, and that in some region of J/t the binding energy becomes positive. Such behavior seems to be natural in the presence of short-range

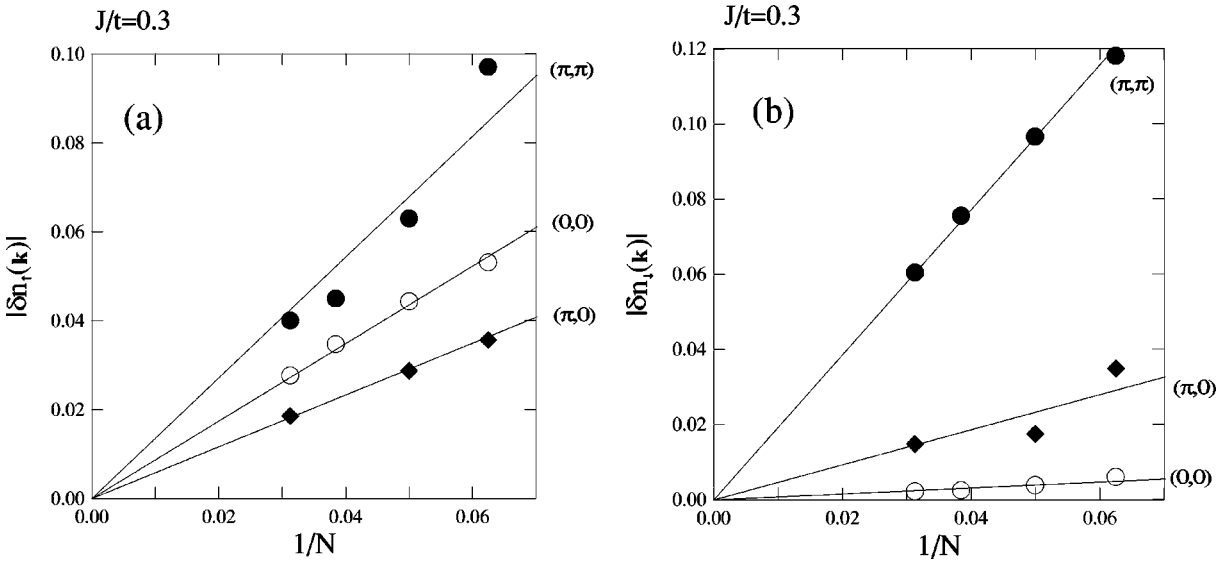

FIG. 3. $1/N$ scaling of the (a) $|\langle \delta n_{\mathbf{k}\uparrow}\rangle|$, (b) $|\langle \delta n_{\mathbf{k}\downarrow}\rangle|$ [see Eq. (3)] for $\mathbf{k}=(\pi,\pi)$ (filled circles), (0,0) (empty circles), and $(\pi,0)$ (filled diamonds) for the single-hole ground state at $J/t=0.3$. The data from 16-, 20-, 26-, and 32-site clusters $[(\pi,\pi)$, (0,0) points] and from 16-, 20-, and 32-site clusters $[(\pi,0)$ point], where these points are available, are used.

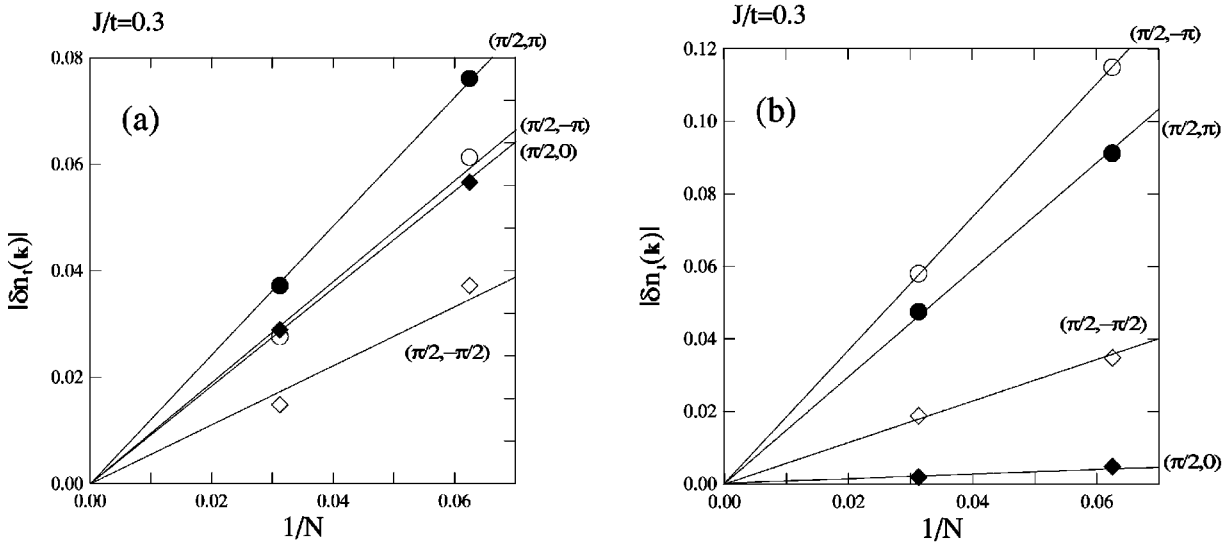

FIG. 4. The same as in Fig. 3 for $\mathbf{k}=(\pi/2,\pi)$ (filled circles), $(\pi/2,-\pi)$ (empty circles), $(\pi/2,0)$ (filled diamonds), and $(\pi/2,-\pi/2)$ (empty diamonds). These points are available from 16- and 32-site clusters only.

attraction between the holes. In this case holes on larger clusters lower their kinetic energy due to delocalization and make the bound state shallower, whereas on smaller ones they are not allowed to move farther apart. Further, holes on smaller clusters are forced to be in the region of the mutual attraction. Since these short-range interactions are believed to be of magnetic origin, the interaction energy has to scale as J. Consequently, the increasing importance of the kinetic energy at small J/t tends to destroy the bound state. This line of thinking leads to a discussion of whether or not the critical threshold of J/t for bound-state formation is above or below the ''realistic'' value of J/t for the cuprates. Attempts have been made to estimate the thermodynamic limit of $(J/t)|_c$ through FSS of the binding energy.[67,69] If we follow the same approach, we obtain the scaling shown in Fig. 6(b), and this data shows the FSS at two representative J/t values. The thermodynamic limit of E_b is negative at the larger J/t (smaller size of the bound state, larger role of the short-range interaction) and positive at the smaller J/t (no bound state).

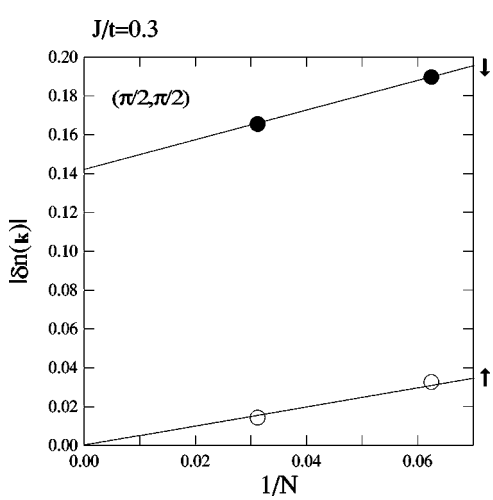

FIG. 5. $1/N$ scaling for the $|\langle \delta n_{\mathbf{k}\uparrow}\rangle|$ (open circles) and $(C+\alpha/N)$ scaling for the dip in $|\langle \delta n_{\mathbf{k}\downarrow}\rangle|$ (filled circles) at the ground-state momentum $\mathbf{k}=\mathbf{P}$, $J/t=0.3$. These points are available for the 16- and 32-site clusters only.

In our opinion, this approach is problematic for at least two reasons. First, there is another important hole-hole interaction, viz. magnon exchange, which also leads to pairing. In fact, it is this interaction that selects the d-wave symmetry state. It has been shown analytically[19,30,36] that this interaction alone leads to the formation of a shallow long-range bound state that does not have a critical value of J/t because the interaction strength grows with t. Therefore, one can expects that further increase in the cluster size will not only lower the kinetic energy of the holes, but will also provide more sites for the holes to take advantage of the long-range attraction. The second reason is the absence of the evident scaling law for the binding energy. Regarding the complexity of the interactions involved and the tendency of the magnetic subsystem towards AF long-range order, we expect different contributions to the FSS of E_b that are of different order in $1/N$ and of comparable magnitudes. This is especially true at smaller J/t when the size of the bound state is comparable to or larger than the cluster size.

Another important quantity that shows further evidence of the hole-hole attraction in an AF background is the hole-hole correlation function $C(r)$, Eq. (2). It has been studied in detail in smaller systems.[44,50,67,69,72] Figures 7(a) and 7(b) show the 32-site ED results for $C(r)$ at $J/t=0.3$ and $J/t=0.8$, respectively. In a wide region of J/t the strongest correlation is at the $\sqrt{2}$ distance, while the nearest-neighbor correlation is also strong. A density-matrix renormalization-group study[78] has also found similar physics. At larger J/t [Fig. 7(b)] the size of the bound state is small: the nearest-neighbor and $\sqrt{2}$ distances accumulate about 80% of the holes. However, at $J/t=0.3$ the *probabilities* of finding the holes at $\sqrt{5}$ and $\sqrt{2}$ distances are almost the same, and only 46% of the holes are located at the nearest-neighbor and $\sqrt{2}$ distances. The correlation decays slowly with distance at small J/t. Hence in the $J/t=0.3$ bound state one can expect $C(r)$ to have a longer ''tail'' in the thermodynamic limit.

The next correlation function that can be used to extract information on the bound state is the EMDF. Figures 8(a),(b) show the EMDF at $J/t=0.3$ and $J/t=1.0$ in the first quad-

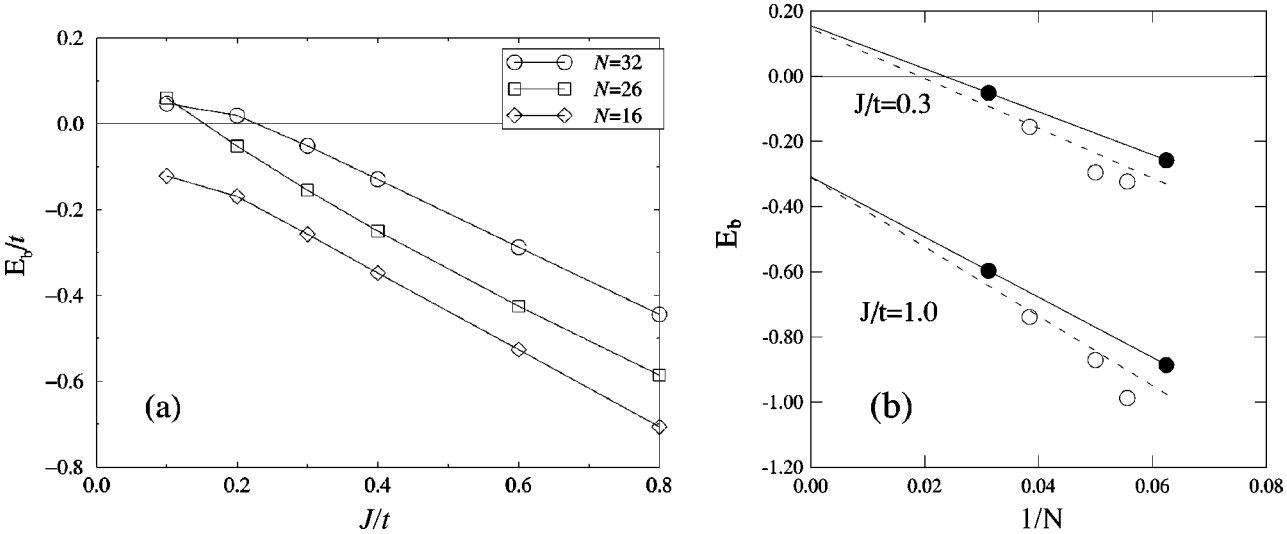

FIG. 6. (a) The J/t dependence of the binding energy E_b, in units of t, from ED studies on the 16- (diamonds), 26- (squares), and 32-site (circles) clusters. (b) The binding energy vs $1/N$ for two representative J/t values, $J/t=0.3$ (upper) and $J/t=1.0$ (lower). The solid and dashed lines are $1/N$ scaling using 16- and 32-site data only (filled circles) and data from all available clusters (open and filled circles), respectively.

rant of the Brillouin zone. Since the total momentum of the system **P** is zero, the EMDF possesses the full square symmetry. Moreover, since the ground state is a singlet, $\langle n_{\mathbf{k}\uparrow}\rangle = \langle n_{\mathbf{k}\downarrow}\rangle = \langle n_{\mathbf{k}}\rangle$. Another noticeable difference from the single-hole EMDF is the absence of a ''dip'' at any **k** point. This is not surprising because one would not expect the holes in the bound state to have a certain momentum. They will be spread over all **k** points especially if the bound state is well localized in real space.

Some of the features of the EMDF are essentially the same as that of the single-hole case. The dome structure is very pronounced. Further, our results shows that the amplitude of the background deviation, $\Delta n = (\langle n_{(0,0)}\rangle - \langle n_{(\pi,\pi)}\rangle)$, is roughly the same as $(\Delta n_{\uparrow}^{1hole} + \Delta n_{\downarrow}^{1hole})$. This shows that the background behavior is due to the single-hole excitations and is irrelevant to the physics of the bound state. We will provide support of this in the next two sections.

In the next section we will show that the important EMDF data are those along the AF Brillouin zone boundary. These data are practically unaffected by the kinematic form factor effect, so they can be used to draw conclusions on the internal structure of the bound state in **k** space. One can interpret the EMDF at these points as the half-filled EMDF suppressed by the hole-occupation number. The hole weight at the single-hole ground-state momentum $(\pi/2,\pi/2)$ is surprisingly small—$\langle n_{\mathbf{k}}\rangle$ deviates from the half-filled value of $\frac{1}{2}$ by only 1%. This is the consequence of the $d_{x^2-y^2}$ symmetry, which restricts the hole weight to be zero at these points. Another interesting feature is that the hole occupation at the $(3\pi/4,\pi/4)$ point is higher than that at $(\pi,0)$ [Fig. 8(a)]. It is worth noting that at smaller J/t the hole occupation numbers at these points are very similar and their absolute values are larger. As follows from the discussion in the next sections, these facts indicate the presence and importance of higher harmonics in the bound state at smaller J/t, because the ''bare'' first d-wave harmonic $[\cos(k_x)-\cos(k_y)]$ will always give a larger hole weight at $(\pi,0)$ than at $(3\pi/4,\pi/4)$.

The available clusters allow us to perform FSS for six of the nine inequivalent **k** points of the 32-site cluster. Results for four of them at $J/t=0.3$ and $J/t=1.0$ are presented in Figs. 9(a),(b). They all show the anticipated $1/N$ scaling. Note that a similar scaling plot at $(\pi/2,\pi/2)$ is not successful because $|\langle \delta n_{\mathbf{k}}\rangle|$ is too small. Figure 10 shows the scaling of the EMDF at $(\pi,0)$. If we discard the 16-site data by arguing that they are spoiled by the artificial degeneracy, one can clearly see the $1/N$ scaling at $J/t=1.0$. In contrast to this, $|\langle \delta n_{(\pi,0)}\rangle|$ at $J/t=0.3$ does not show the same $1/N$ scaling. We attribute these different behaviors to the different sizes of the bound states. The $J/t=1.0$ bound state is small. Therefore, it has to scale as $1/N$ even when N is not too large. The $J/t=0.3$ bound state is relatively large. An increase in the cluster size redistributes the hole weight among the new harmonics that become available in larger systems. The EMDF at those points not along the AFBZ boundary [Figs. 9(a),(b)] mostly result from kinematic effects that are saturated at shorter distances. Therefore, they do not depend much on the details of the bound-state structure.

IV. ANALYTICAL RESULTS

Studies of the doped t-J model via the ED technique provide important information on effective quasiparticle theories. However, these same numerical results also posed some problems and made questionable the relation of these analytical studies to the problem of the ''finite doping of the finite system.'' For example, the EMDF for the ground states of the different number of holes and the pair-correlation function for the two holes doped into the system were intensively studied numerically (see Secs. II A, III). It turned out that the results for these quantities were found to be in contradiction to some expectations. EMDF, which was naively expected to show something like ''hole pockets,'' or simply hole-rich and electron-rich regions in **k** space, demonstrates a dramatic deviation of this quantity for the doped clusters from the half-filled (no holes) case with the strong variation

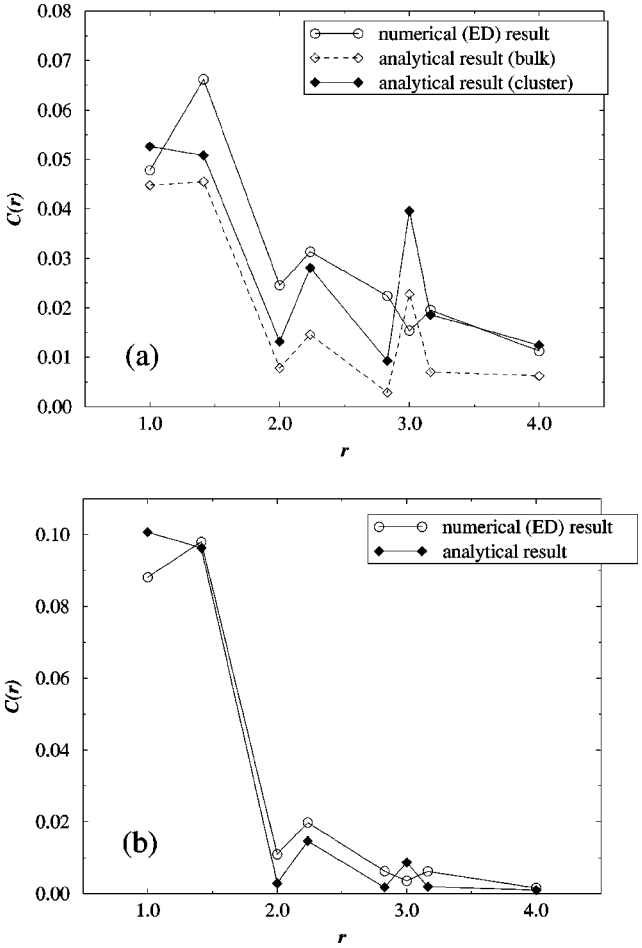

FIG. 7. The spatial correlation function, $C(r)$, for two holes doped into a square lattice described by the t-J model, for (a) $J/t=0.3$, and (b) $J/t=1.0$. Our ED results (open circles), the analytical results for an infinite square lattice (open diamonds), and the analytical results mapped onto a 32-site square lattice (filled diamonds), are all shown. The lines are guides to the eye. In (b), analytical results for the cluster are very close to those for the bulk, and hence are not shown.

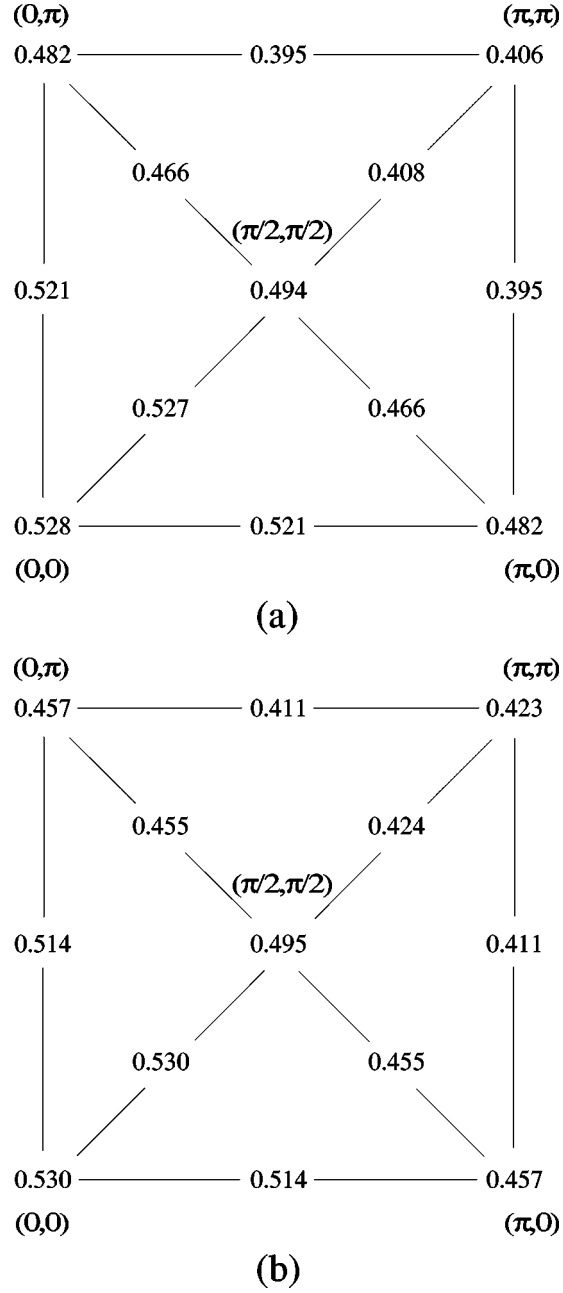

FIG. 8. The EMDF for the two-hole ground state, $\mathbf{P}=0$, $S^z_{tot}=0$ at (a) $J/t=0.3$, (b) $J/t=1.0$ within the first quadrant of the BZ.

across the whole Brillouin zone. Moreover, there is a strong doping dependence of these results. Data for the two-hole ground state differ significantly from the single-hole ones. More surprisingly, the overall shape of the EMDF reminds one of the free electrons with a nearest-neighbor hopping band. This was the reason for the conjecture that the t-J model already at rather low doping concentration undergoes a transition to the free-electron physics and shows a ''large'' Fermi surface.[57] Also, the hole-hole correlation function for the d-wave bound state shows the largest weight of the holes in the configurations that should be forbidden by the d-wave symmetry (the so-called $\sqrt{2}$-paradox). In this situation, a physical explanation of such puzzling behavior of the correlation functions together with an analytical picture would be highly desirable.

A qualitative understanding of these effects in the context of the spin-polaron physics has been achieved in the works of Eder and Becker,[15] and Eder and Wróbel,[16] wherein the authors showed that the t-J model quasiparticles will favor qualitatively the same EMDF as the ones found in the numerical calculations. Using rather general arguments, they demonstrated that the ''large Fermi surface'' is a consequence of simple sum rules and a minimum of the total energy, and it is completely irrelevant to the problem of the real Fermi-surface identification. The main idea of these works is that the hole pockets should be attributed to the quasiparticles, not to the bare holes. Since the renormalization is strong only a relatively small part of the polaron can be visualized in $\mathbf{k}$ space as a fermion having a certain momentum. The ''dressed'' part of the spin polaron is responsible for the background in the EMDF, which is spread over the entire BZ. More specifically, the EMDF does not only measure the lack of the electrons due to the center of the polaron, but it also keeps track of the hole distribution inside the polaron. Similar physics has been discussed recently in Ref. 18.

Within the same theoretical framework, i.e., a variational

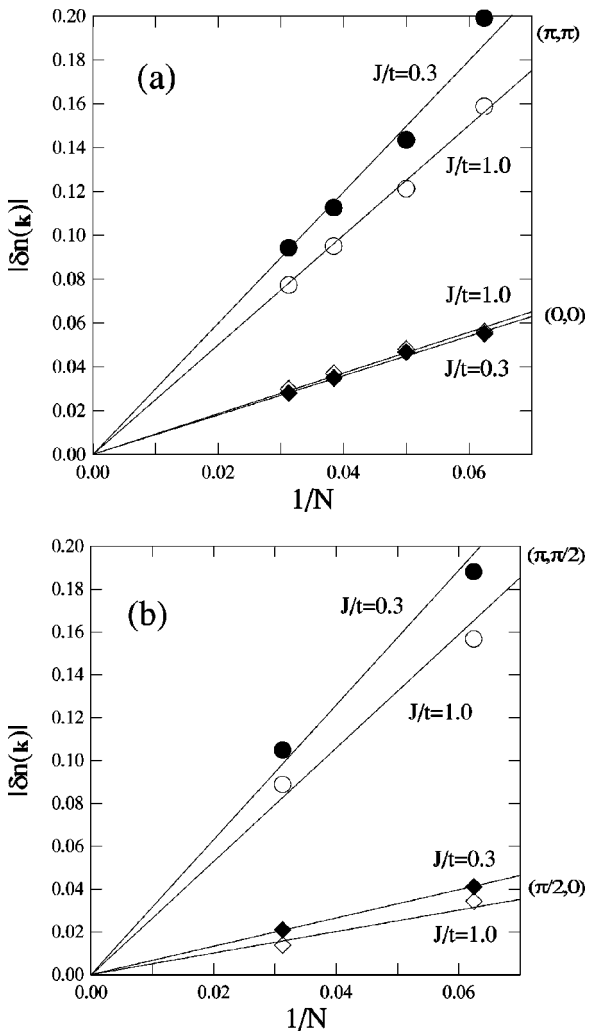

FIG. 9. $1/N$ scaling of the $|\langle \delta n_{\mathbf{k}} \rangle|$ in the two-hole ground state, for (a) $\mathbf{k}=(\pi,\pi)$ at $J/t=0.3$ (filled circles) and $J/t=1.0$ (empty circles), and (0,0) at $J/t=0.3$ (filled diamonds) and $J/t=1.0$ (empty diamonds), and (b) $\mathbf{k}=(\pi,\pi/2)$ at $J/t=0.3$ (filled circles) and $J/t=1.0$ (empty circles), and $(\pi/2,0)$ at $J/t=0.3$ (filled diamonds) and $J/t=1.0$ (empty diamonds).

string approach, we mention that the pairing problem for two holes has been considered elsewhere[17] and the source of the large probability of finding holes in the ground state along the diagonal of an elementary square can be explained by the large weight of the ''hole×(hole+1 spin flip)'' combination in the two-hole *d*-wave bound-state wave function. Qualitative discussion of the same physics has been done recently in Ref. 79.

In what follows we will show how the qualitative picture drawn in Refs. 15–17, which gives a basic understanding of the numerical data, can be reproduced using simple ansatzes for the spin polarons and their bound state. Then, the CT approach is used to derive analytical expressions that are able to explain *quantitatively* most of the one- and two-hole ED data for the ground states described in Sec. II, and earlier in the literature.

A. Qualitative analysis using a simplified model

We begin our analytical calculations of two holes described by the *t*-*J* model by considering a simplified treatment of two holes moving in an antiferromagnetic (AFM) Ising background. We then evaluate the EMDF and $C(r)$ using this simplified model in order to see what kind of behavior one can expect in the ground state of spin polarons. This work is instructive, and helps in understanding this problem. So we present these preliminary results first.

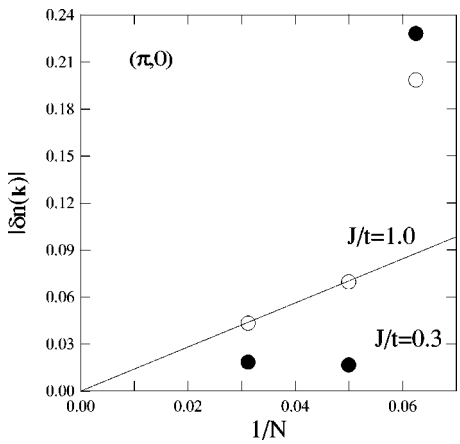

FIG. 10. $|\langle \delta n_{\mathbf{k}} \rangle|$ in the two-hole ground state vs $1/N$ for $\mathbf{k}=(\pi,0)$ at $J/t=0.3$ (filled circles) and $J/t=1.0$ (empty circles). Solid line shows $1/N$ scaling for the $J/t=1.0$ data if the 16-site cluster result is ignored.

Consider the EMDF. In a system without holes, one finds that $\langle n_{\mathbf{k}\sigma} \rangle = 1/2$ everywhere in the full Brillouin zone. This is a consequence of the purely local character of the electronic states and $S^z_{tot}=0$. By definition

$$\langle n_{\mathbf{k}\sigma} \rangle = 1/N \, \Sigma_{ij} e^{i\mathbf{k}\mathbf{r}_{ij}} \langle \tilde{c}^{\dagger}_{i\sigma} \tilde{c}_{j\sigma} \rangle$$
$$= 1/N \, \Sigma_i \langle \tilde{c}^{\dagger}_{i\sigma} \tilde{c}_{i\sigma} \rangle + 1/N \, \Sigma_{i,d\neq 0} e^{i\mathbf{k}\cdot\mathbf{d}} \langle \tilde{c}^{\dagger}_{i\sigma} \tilde{c}_{i+d\sigma} \rangle .$$

The second term is zero for the half-filled case and the first term yields $\langle n_{\mathbf{k}\uparrow} \rangle = \langle n_{\mathbf{k}\downarrow} \rangle = 1/2$. An informative result that follows from the second term is that hole doping makes the matrix elements between different ''strings'' of the polaron wave function nonzero, and accompanied by the phase factor $e^{i\mathbf{k}\cdot\mathbf{d}}$, where $|\mathbf{d}|$ is the difference between the lengths of the strings. For example, the matrix element between the bare component $(\Sigma_i \tilde{c}_{i\downarrow} e^{i\mathbf{k}\mathbf{r}_i}|0\rangle)$ and the one spin-flip string component $(\Sigma_{i,\delta} S^+_i \tilde{c}_{i+\delta\uparrow} e^{i\mathbf{k}\mathbf{r}_i}|0\rangle)$ is proportional to $\Sigma_\delta e^{i\mathbf{k}\boldsymbol{\delta}} \sim \gamma_{\mathbf{k}}$, which is asymmetric with respect to the transformation $\mathbf{k} \to \mathbf{k}+(\pi,\pi)$, $\gamma_{\mathbf{k}} = -\gamma_{\mathbf{k}+\mathbf{Q}}$. Thus all odd-distance matrix elements are responsible for the antisymmetric contribution to $\langle n_{\mathbf{k}} \rangle$, and this asymmetry makes $\langle n_{\mathbf{k}} \rangle$ resemble the shape of a large Fermi surface. Note, that this unusual effect is closely related to the localized character of the electronic states and the spin polaron nature of the carriers. Recently, a similar asymmetry observed in the angle-resolved photoemission spectroscopy data of an undoped ($Sr_2CuO_2Cl_2$) (Ref. 80) and doped[18] AFM insulators has been successfully explained using essentially the same ideas.

Hole excitations near half-filling (when long-range AFM order is present) are most concisely explained using the spinless-hole Schwinger-boson representation for the constrained fermion operators. Thus it is necessary to express

$\langle n_{\mathbf{k}}\rangle$ and $C(r)$ in terms of averages of combinations of the hole and magnon operators. The essence of this representation is the following. The creation of a hole (annihilation of an electron) at site i in sublattice $A=\{\uparrow\}$ (with the main direction of the spins being up) is achieved by operating $\tilde{c}_{i\uparrow}$ on the ground state. Thus, $\tilde{c}_{i\uparrow}\simeq h_i^\dagger$. The action of the same operator on site j in sublattice $B=\{\downarrow\}$ is nonzero only if the spin is in the ''wrong'' direction ($\uparrow$). Therefore, creation of a hole is accompanied by the annihilation of a spin excitation: $\tilde{c}_{j\uparrow}=h_j^\dagger S_j^- \simeq h_j^\dagger a_j$. Thus,

$$\begin{aligned}\langle \tilde{c}_{i\uparrow}^\dagger \tilde{c}_{j\uparrow}\rangle &= \langle h_{A,i} h_{A,j}^\dagger (1-a_{A,j}^\dagger a_{A,j})\rangle \delta_{i,A}\delta_{j,A} \\ &+ \langle h_{A,i} h_{B,j}^\dagger a_{B,j}\rangle \delta_{i,A}\delta_{j,B} + \langle h_{B,i} a_{B,j}^\dagger h_{A,j}^\dagger\rangle \delta_{i,B}\delta_{j,A} \\ &+ \langle h_{B,i} h_{B,j}^\dagger a_{B,j}^\dagger a_{B,j}\rangle \delta_{i,B}\delta_{j,B}. \end{aligned} \tag{6}$$

The above will suffice for the description in this paper—for an advanced and detailed discussion of this representation we refer the readers to Ref. 81.

First we examine a simple ansatz for the single-hole ground-state wave function[27,41]

$$\begin{aligned}|1\rangle &= \sqrt{\frac{2}{N}}\tilde{h}_{B,\mathbf{P}}^\dagger |0\rangle \\ &= \sqrt{\frac{2}{N}}\left[\alpha h_{B,\mathbf{P}}^\dagger + 4\beta \sum_{\mathbf{q}} \gamma_{\mathbf{P}-\mathbf{q}} h_{A,\mathbf{P}-\mathbf{q}}^\dagger a_{B,\mathbf{q}}^\dagger\right]|0\rangle, \end{aligned} \tag{7}$$

where $\alpha^2+4\beta^2=1$, and, as noted in Ref. 15, the sign of the term linear in $\gamma_{\mathbf{k}}$ is found from minimizing the kinetic energy. (Note that the origin of the hole is in sublattice B, so the total spin of the system is $S_{tot}^z=1/2$.) Hereafter, $\mathbf{q}\in ABZ$,

$$\sum_{\mathbf{q}} = \frac{2}{N}\sum_{q_n,n=1}^{N/2},$$

and

$$\{h_{A(B)\mathbf{k}}, h_{A(B)\mathbf{k}'}^\dagger\} = [a_{A(B)\mathbf{k}}, a_{A(B)\mathbf{k}'}^\dagger] = \delta_{\mathbf{k},\mathbf{k}'}\cdot N/2. \tag{8}$$

Minimal algebra for the EMDF and $C(r)$ yields

$$\begin{aligned}\langle n_{\mathbf{k}\uparrow}\rangle N &\simeq \frac{N}{2} - \langle h_{A,\mathbf{k}}^\dagger h_{A,\mathbf{k}}\rangle + \sum_{\mathbf{q}} (\langle a_{B,\mathbf{q}}^\dagger a_{B,\mathbf{q}}\rangle - \langle a_{A,\mathbf{q}}^\dagger a_{A,\mathbf{q}}\rangle) \\ &- \left(\left\langle h_{A,\mathbf{k}}^\dagger \sum_{\mathbf{q}} h_{B,\mathbf{k}+\mathbf{q}} a_{B,\mathbf{q}}^\dagger\right\rangle + \text{H.c.}\right), \\ \langle n_{\mathbf{k}\downarrow}\rangle N &\simeq \frac{N}{2} - \langle h_{B,\mathbf{k}}^\dagger h_{B,\mathbf{k}}\rangle + \sum_{\mathbf{q}} (\langle a_{A,\mathbf{q}}^\dagger a_{A,\mathbf{q}}\rangle - \langle a_{B,\mathbf{q}}^\dagger a_{B,\mathbf{q}}\rangle) \\ &- \left(\left\langle h_{B,\mathbf{k}}^\dagger \sum_{\mathbf{q}} h_{A,\mathbf{k}+\mathbf{q}} a_{A,\mathbf{q}}^\dagger\right\rangle + \text{H.c.}\right), \\ C(r) &= \frac{1}{N_h N_E(r)}\sum_{i,j} \langle n_i^h n_j^h \delta_{|i-j|,r}\rangle, \end{aligned} \tag{9}$$

where $n_i^h = h_i^\dagger h_i$ is the hole number operator. The physical meanings of the terms in $\langle n_{\mathbf{k}}\rangle$ are apparent. The number of electrons with spin up and momentum $\mathbf{k}$ is reduced by the amount of holes having the same momentum and by the spin flips in sublattice A. It is increased by the number of spin excitations in sublattice B. The last term is not zero between different components of the spin-polaron wave function, reflecting the inner structure of this quasiparticle, or the kinematic ''form factor.'' Alternatively, according to Ref. 15, it reflects ''the fast movement of the hole inside the bag.''

Using $|1\rangle$ from Eq. (7), Eq. (9) gives

$$\langle n_{\mathbf{k}\uparrow}\rangle \simeq \frac{1}{2} + \frac{1}{N}(-16\beta^2\gamma_{\mathbf{k}}^2 + 4\beta^2 + 8|\alpha\beta|\gamma_{\mathbf{k}}), \tag{10}$$

$$\langle n_{\mathbf{k}\downarrow}\rangle \simeq \frac{1}{2} - \frac{1}{2}\alpha^2\delta_{\mathbf{k},\mathbf{P}} - \frac{1}{N}4\beta^2.$$

These simple expressions already contain significant qualitative information about the EMDF for the single-hole ground state. There is a dip in $\langle n_{\mathbf{k}\downarrow}\rangle$ at $\mathbf{k}=\mathbf{P}$ with weight equal to one-half of the quasiparticle residue, corresponding to the center of the polaron. There is also a constant positive (negative) shift in $\langle n_{\mathbf{k}\uparrow}\rangle$ ($\langle n_{\mathbf{k}\downarrow}\rangle$) due to spin excitations in sublattice B [see Eq. (7)]. Although $\langle n_{\mathbf{k}\uparrow}\rangle$ does not have any dips, it does have two other features. One is due to the hole distribution in the dressed part of the polaron ($\sim\gamma_{\mathbf{k}}^2$), and the other is due to the ''interstring'' matrix elements ($\sim\gamma_{\mathbf{k}}$). The absence of the interstring terms in $\langle n_{\mathbf{k}\downarrow}\rangle$ in Eq. (10) is due to the approximation made in the above ansatz viz. Eq. (7), namely, the elimination of the longer strings that are necessary to produce the ''dome'' structure of $\langle n_{\mathbf{k}\downarrow}\rangle$. This explains the smaller amplitude and stronger t/J dependence of the difference $\Delta n_\downarrow = n_{(0,0)\downarrow} - n_{(\pi,\pi)\downarrow}$ than those of $\Delta n_\uparrow$ for the single-hole ground state.

Thus, most features of the single-hole EMDF data reported in Sec. III can be understood using this simplified model. According to Eq. (10) all $\langle \delta n_{\mathbf{k}\sigma}\rangle$ scale as $1/N$ except for the dip that scales as $C+\alpha/N$, a result that is employed in the FSS analysis of the ED numerical work.

In order to carry out a similar analysis for the two-hole case, one has to solve the Schrödinger equation for the bound-state problem. Instead of doing this we simply propose the nearest-neighbor bound state wave function having d-wave symmetry and $S_{tot}^z=0$ based on the expectation that two static holes attract each other through the ''sharing common link'' effect (viz., $H_{int}=-J/2\ \ n_i^h n_j^h$):

$$\begin{aligned}|2\rangle &= \sqrt{\frac{2}{N}}\sum_{\mathbf{p}} \Delta_{\mathbf{p}}^d \tilde{h}_{A,\mathbf{p}}^\dagger \tilde{h}_{B,-\mathbf{p}}^\dagger |0\rangle \\ &= \sqrt{\frac{2}{N}}\sum_{\mathbf{p}} \Delta_{\mathbf{p}}^d \Bigg[\alpha^2 h_{A,\mathbf{p}}^\dagger h_{B,-\mathbf{p}}^\dagger \\ &+ 4\alpha\beta\sum_{\mathbf{q}} (\gamma_{\mathbf{p}-\mathbf{q}} h_{B,\mathbf{p}-\mathbf{q}}^\dagger h_{B,-\mathbf{p}}^\dagger a_{A,\mathbf{q}}^\dagger \\ &+ \gamma_{-\mathbf{p}-\mathbf{q}} h_{A,\mathbf{p}}^\dagger h_{A,-\mathbf{p}-\mathbf{q}}^\dagger a_{B,\mathbf{q}}^\dagger) \\ &+ 16\beta^2\sum_{\mathbf{q},\mathbf{q}'} \gamma_{\mathbf{p}-\mathbf{q}}\gamma_{-\mathbf{p}-\mathbf{q}'} h_{B,\mathbf{p}-\mathbf{q}}^\dagger h_{A,-\mathbf{p}-\mathbf{q}}^\dagger a_{A,\mathbf{q}}^\dagger a_{B,\mathbf{q}'}^\dagger\Bigg]|0\rangle, \end{aligned} \tag{11}$$

with $\Delta_{\mathbf{p}}^d = [\cos(p_x) - \cos(p_y)]$ ensuring that the centers of the polarons are at the nearest-neighbor sites.

The EMDF calculation using $|2\rangle$ in Eq. (11) yields

$$\langle n_{\mathbf{k}}\rangle=\langle n_{\mathbf{k}\uparrow}\rangle=\langle n_{\mathbf{k}\downarrow}\rangle \simeq\frac{1}{2}+\frac{1}{N}(-\alpha^2(\Delta_{\mathbf{k}}^d)^2-16\beta^2\gamma_{\mathbf{k}}^2+8|\alpha\beta|\gamma_{\mathbf{k}}), \quad (12)$$

where the terms inside the bracket are simply the sum of the $1/N$ terms in the $\langle n_{\mathbf{k}\uparrow}\rangle$ and $\langle n_{\mathbf{k}\downarrow}\rangle$ expressions of Eq. (10) for the single-hole case, and the dip structure is replaced by the probability of finding a bare hole with momentum $\mathbf{k}$ in the bound state. This explains the observation mentioned in Sec. III that the quantity $\Delta n=n_{(0,0)}-n_{(\pi,\pi)}$ for the two-hole case is roughly the same as $\Delta n_\uparrow+\Delta n_\downarrow$ for the single-hole case. It is interesting to note that since the $\mathbf{k}$ dependence of the terms from the dressed part of the polaron and from the ''inter-string'' processes vanish at the boundary of the magnetic Brillouin zone ($\gamma_{\mathbf{k}}=0$), features of the EMDF along this line are not disguised by kinematic effects. Thus, one can directly observe the structure of the bound state wave function $\Delta_{\mathbf{k}}^d$ from the $\langle n_{\mathbf{k}}\rangle$ data at these points. In particular, the $(\pi/2,\pi/2)$ point has to have zero hole weight due to the d-wave symmetry of the bound state. For the particular form of $\Delta_{\mathbf{p}}^d$ we have chosen, the maximum of the hole weight (minimum in $\langle n_{\mathbf{k}}\rangle$) will be at the $(\pi,0)$ point.

The hole-hole correlation function on different clusters consistently shows a maximal probability for states in which the holes are along the diagonal of an elementary square, i.e., they prefer to be at a distance $\sqrt{2}a$ from one another, where a is the lattice constant. [At first glance, such a configuration should be forbidden by the $d_{x^2-y^2}$ symmetry of the state. One way to resolve this paradox, as suggested by Poilblanc,[68] is to introduce modified creation pair operators $h_i^\dagger h_{i\pm x\pm y}^\dagger S_{i\pm x(y)}^+$ to the bare $h_i^\dagger h_{i\pm x(y)}^\dagger$ pair operator. It is clear that the bound-state wave function Eq. (11) includes such combinations naturally.] Calculation of $C(r)$ of Eq. (9) in the ground state given by Eq. (11) gives

$$C(1)=\alpha^4/4+9\beta^4/4,\quad C(\sqrt{2})=\alpha^2\beta^2,$$

$$C(2)=\alpha^2\beta^2/2,\quad C(\sqrt{5})=3\beta^4/4,\quad C(3)=\beta^4/4. \quad (13)$$

For the physical range of $t/J\sim 2-3$ the weights accumulated in the bare and ''one-string'' parts of the polaron wave function are almost identical, $\alpha^2\simeq 4\beta^2$.[27,38] This gives $C(1)\simeq C(\sqrt{2})$, in qualitative agreement with the numerical results.

Thus, one can conclude that our simple considerations of one and two holes in a system of Ising spins, based on a simplified spin-polaron picture, already shows qualitative agreement with the numerical data. The treatment of the realistic system with a Néel spin background requires a proper account of the spin fluctuations, the long-range dynamics of the system, and multiple spin excitations (longer strings).

B. CT approach

1. CT Hamiltonian

The t-J model Hamiltonian (1) can be rewritten using the spinless-fermion representation for the constrained fermion operators and Holstein-Primakoff[12,14] or Dyson-Maleev[81] representation for the spin operators. These formalisms have been shown to be adequate in treating the nonlinear feature of the kinetic energy term of Eq. (1) properly. Subsequent diagonalization of the spin part of the Hamiltonian by the Bogoliubov transformation naturally includes spin fluctuations in the ground state.

The essential part of the t-J Hamiltonian rewritten in this way looks like the electron-phonon Hamiltonian for the ''usual'' polaron problem with an additional direct fermion-fermion interaction term:

$$\mathcal{H}_{t-J}\simeq\sum_{\mathbf{q}}\omega_{\mathbf{q}}\alpha_{\mathbf{q}}^\dagger\alpha_{\mathbf{q}}+\sum_{\mathbf{k},\mathbf{q}}(M_{\mathbf{k},\mathbf{q}}h_{\mathbf{k}-\mathbf{q}}^\dagger h_{\mathbf{k}}\alpha_{\mathbf{q}}^\dagger+\text{H.c.})+\Delta H,$$

$$\Delta H=-2J(1-2\lambda)\sum_{\mathbf{k},\mathbf{k}',\mathbf{q}}\gamma_{\mathbf{q}}h_{\mathbf{k}-\mathbf{q}}^\dagger h_{\mathbf{k}'+q}^\dagger h_{\mathbf{k}'}h_{\mathbf{k}}, \quad (14)$$

where $h^\dagger(h),\alpha^\dagger(\alpha)$, are the spinless hole and magnon operators, respectively, $\omega_{\mathbf{q}}=2J(1-\gamma_{\mathbf{q}}^2)^{1/2}$ is the spin-wave energy, $M_{\mathbf{k},\mathbf{q}}=4t(\gamma_{\mathbf{k}-\mathbf{q}}U_{\mathbf{q}}+\gamma_{\mathbf{k}}V_{\mathbf{q}})$, $U_{\mathbf{q}},V_{\mathbf{q}}$ are the Bogoliubov transformation parameters, $\gamma_{\mathbf{k}}=(\cos k_x+\cos k_y)/2$, $\lambda=\Sigma_{\mathbf{q}}(V_{\mathbf{q}}^2-\gamma_{\mathbf{q}}U_{\mathbf{q}}V_{\mathbf{q}})=-0.08$. ΔH is an effective hole-hole attraction due to minimization of the number of broken AF bonds. Two important differences make the t-J version of the polaron problem much more difficult to study: (i) the absence of bare dispersion term of the hole,[82] and (ii) the essentially nonlocal character of the hole-magnon interaction, because each process of emitting (absorbing) a magnon is associated with an intersite hole hopping.

The CT approach has been applied to the spin-polaron Hamiltonian of Eq. (14) in Ref. 19. The generator of the CT was proposed to be in the form

$$\mathcal{S}=\sum_{\mathbf{k},\mathbf{q}}f_{\mathbf{k}}M_{\mathbf{k},\mathbf{q}}(h_{\mathbf{k}-\mathbf{q}}^\dagger h_{\mathbf{k}}\alpha_{\mathbf{q}}^\dagger-\text{H.c.}), \quad (15)$$

where $f_{\mathbf{k}}$ is the parameter of the transformation, and in Ref. 19 $f_{\mathbf{k}}$ was chosen to minimize the single-hole energy, viz.

$$\frac{\delta}{\delta f_{\mathbf{k}}}\left(\sum_{\mathbf{k}'}E_{\mathbf{k}'}\right)=0. \quad (16)$$

The negligible role of the higher-order hole-magnon vertices in the transformed Hamiltonian was demonstrated and it was argued that the initially strong hole-magnon interaction in Eq. (14) is transfered mainly into a hole ''dressing'' and into the hole-hole interaction. Thus, for a wide region of t/J one can restrict one's considerations to the effective Hamiltonian

$$\mathcal{H}_{eff}=\sum_{\mathbf{k}}E_{\mathbf{k}}\tilde{h}_{\mathbf{k}}^\dagger\tilde{h}_{\mathbf{k}}+\sum_{\mathbf{q}}\omega_{\mathbf{q}}\alpha_{\mathbf{q}}^\dagger\alpha_{\mathbf{q}}+\sum_{\mathbf{k},\mathbf{k}',\mathbf{q}}V_{\mathbf{k},\mathbf{k}',\mathbf{q}}\tilde{h}_{\mathbf{k}-\mathbf{q}}^\dagger\tilde{h}_{\mathbf{k}'+q}^\dagger\tilde{h}_{\mathbf{k}'}\tilde{h}_{\mathbf{k}}+\sum_{\mathbf{k},\mathbf{q}}F_{\mathbf{k},\mathbf{q}}M_{\mathbf{k},\mathbf{q}}(\tilde{h}_{\mathbf{k}-\mathbf{q}}^\dagger\tilde{h}_{\mathbf{k}}\alpha_{\mathbf{q}}^\dagger+\text{H.c.}), \quad (17)$$

where $E_{\mathbf{k}}$ and $\omega_{\mathbf{q}}$ are the polaron and magnon energies, respectively, $V_{\mathbf{k},\mathbf{k}',\mathbf{q}}$ is the direct polaron-polaron interaction, $M_{\mathbf{k},\mathbf{q}}$ is the bare hole-magnon vertex, and $F_{\mathbf{k},\mathbf{q}}$ is the renormalization form factor that is close to zero at large $\mathbf{q}$, and is constant ($\sim 0.2-0.4$) at small $\mathbf{q}$. The last term, which cor-

responds to the interaction of the hole with long-range spin waves, has been left in the effective Hamiltonian in this form to account for the retardation effect in the polaron-polaron spin-wave exchange. Also, short-range spin-wave exchange has been converted to the direct polaron-polaron interaction. The polaron energy $E_{\mathbf{k}}$ and the weights of the components of the polaron's wave function have been compared with the results of the other works, especially SCBA results, and very good agreements were found. Since the derivation of the single polaron energy *and* the polaron-polaron interaction in the framework of CT approach are the same, one can hope that the effective Hamiltonian of Eq. (17) properly describes the interaction between the low-energy excitations of the t-J model.

2. Our calculations using the CT approach

We are interested in the ground state with total spin $S^z_{tot}=1/2$ $(S^z_{tot}=0)$ for the single-hole (two-hole) case in an AF ordered system. Thus, it is necessary to use a two-sublattice representation for the fermions and bosons.[19] In the two-sublattice representation there are two types of holes and magnons, both defined inside the first magnetic Brillouin zone, whereas in the one-sublattice representations holes and magnons are defined inside the full Brillouin zone. In the previous subsection we used the latter for the sake of simplifying notations. There is a simple relation between these two representations:

$$h_{\mathbf{k}}=(f_{\mathbf{k}}+g_{\mathbf{k}})/\sqrt{2},\quad h_{\mathbf{k}+(\pi,\pi)}=(f_{\mathbf{k}}-g_{\mathbf{k}})/\sqrt{2},$$
$$a_{\mathbf{q}}=(\alpha_{\mathbf{q}}+\beta_{\mathbf{q}})/\sqrt{2},\quad a_{\mathbf{q}+(\pi,\pi)}=(\alpha_{\mathbf{q}}-\beta_{\mathbf{q}})/\sqrt{2}, \tag{18}$$

where $f_{\mathbf{k}}$ and $g_{\mathbf{k}}$ correspond to the hole excitations in the A and B sublattices, respectively. $\alpha_{\mathbf{q}}$ and $\beta_{\mathbf{q}}$ are the two branches of the Bogoliubov spin-wave excitations.

The correlation functions $\langle n_{\mathbf{k}\sigma}\rangle$ and $C(r)$ expressed in terms of the averages of the hole and magnon operators are

$$\begin{aligned}\langle n_{\mathbf{k}\uparrow}\rangle N\simeq&\frac{N}{2}-(1-\delta\lambda)\langle f^\dagger_{\mathbf{k}}f_{\mathbf{k}}\rangle-\sum_{\mathbf{q}}\langle g^\dagger_{\mathbf{k}+\mathbf{q}}g_{\mathbf{k}+\mathbf{q}}\rangle V^2_{\mathbf{q}}\\&+\sum_{\mathbf{q}}(\langle\beta^\dagger_{\mathbf{q}}\beta_{\mathbf{q}}\rangle-\langle\alpha^\dagger_{\mathbf{q}}\alpha_{\mathbf{q}}\rangle)\\&-\left(\left\langle f^\dagger_{\mathbf{k}}\sum_{\mathbf{q}}g_{\mathbf{k}+\mathbf{q}}(\beta^\dagger_{\mathbf{q}}U_{\mathbf{q}}+\alpha_{-\mathbf{q}}V_{\mathbf{q}})\right\rangle+\text{H.c.}\right),\\\langle n_{\mathbf{k}\downarrow}\rangle N\simeq&\frac{N}{2}-(1-\delta\lambda)\langle g^\dagger_{\mathbf{k}}g_{\mathbf{k}}\rangle-\sum_{\mathbf{q}}\langle f^\dagger_{\mathbf{k}+\mathbf{q}}f_{\mathbf{k}+\mathbf{q}}\rangle V^2_{\mathbf{q}}\\&+\sum_{\mathbf{q}}(\langle\alpha^\dagger_{\mathbf{q}}\alpha_{\mathbf{q}}\rangle-\langle\beta^\dagger_{\mathbf{q}}\beta_{\mathbf{q}}\rangle)\\&-\left(\left\langle g^\dagger_{\mathbf{k}}\sum_{\mathbf{q}}f_{\mathbf{k}+\mathbf{q}}(\alpha^\dagger_{\mathbf{q}}U_{\mathbf{q}}+\beta_{-\mathbf{q}}V_{\mathbf{q}})\right\rangle+\text{H.c.}\right),\\C(r)=&\frac{1}{N_hN_E(r)}\sum_{i,j}\langle n^h_i n^h_j\delta_{|i-j|,r}\rangle,\quad h=f(g),\\&\text{when}\quad i\in\{A\}(\{B\}),\end{aligned}\tag{19}$$

where $\delta\lambda=\Sigma_{\mathbf{q}}V^2_{\mathbf{q}}=0.19$. The negligible contribution of the higher-order terms (in the number of magnons) to $\langle n_{\mathbf{k},\sigma}\rangle$ has been checked and these terms are omitted.

It is interesting to compare these expressions with those for the Ising limit of the model given in Eq. (10). The number of holes in sublattice A reducing the number of electrons with spin up is decreased by the spin fluctuations ($\delta\lambda$, first term), but due to the same effect the reduction in $\langle n_{\mathbf{k}\uparrow}\rangle$ can be done by the holes in the sublattice B (second term). The third terms take into account an imbalance of the number of spin excitations of different types. The last term is nonzero for the interstring processes (now strings are just the components of the wave function with the spin excitations).

Using the CT generator of Eq. (15) one obtains the wave function of the spin polaron ($S^z_{tot}=+1/2$):

$$\begin{aligned}|1\rangle=&\sqrt{\frac{2}{N}}\tilde{g}^\dagger_{\mathbf{P}}|0\rangle=\sqrt{\frac{2}{N}}e^{\mathcal{S}}g^\dagger_{\mathbf{P}}|0\rangle\\=&\sqrt{\frac{2}{N}}\Bigg[a_{\mathbf{P}}g^\dagger_{\mathbf{P}}+\sum_{\mathbf{q}}b_{\mathbf{P},\mathbf{q}}f^\dagger_{\mathbf{P}-\mathbf{q}}\beta^\dagger_{\mathbf{q}}\\&+\sum_{\mathbf{q},\mathbf{q}'}c_{\mathbf{P},\mathbf{q},\mathbf{q}'}g^\dagger_{\mathbf{P}-\mathbf{q}-\mathbf{q}'}\beta^\dagger_{\mathbf{q}}\alpha^\dagger_{\mathbf{q}'}+\cdots\Bigg]|0\rangle.\end{aligned}\tag{20}$$

Here, $a^2_{\mathbf{P}}=Z_{\mathbf{P}}<1$ is the quasiparticle residue. An explicit expression for the exact spin-polaron wave function within the SCBA was written in Ref. 24 in the same form. The ground-state momenta for the spin-polaron in the pure t-J model are $\pm(\pm\pi/2,\pi/2)$.

Then, using Eq. (20) the single-hole EMDF is found to be given as

$$\begin{aligned}\langle n_{\mathbf{k}\uparrow}\rangle\simeq&\frac{1}{2}+\frac{1}{N}\Bigg(-(1-\delta\lambda)b^2_{\mathbf{P},\mathbf{P}-\mathbf{k}}-a^2_{\mathbf{P}}V^2_{\mathbf{P}-\mathbf{k}}\\&-\sum_{\mathbf{q},\mathbf{q}'}c^2_{\mathbf{P},\mathbf{q}',\mathbf{P}-\mathbf{k}-\mathbf{q}-\mathbf{q}'}V^2_{\mathbf{q}}+\sum_{\mathbf{q}}b^2_{\mathbf{P},\mathbf{q}}\\&-2\left(a_{\mathbf{P}}b_{\mathbf{P},\mathbf{P}-\mathbf{k}}U_{\mathbf{P}-\mathbf{k}}+b_{\mathbf{P},\mathbf{P}-\mathbf{k}}\sum_{\mathbf{q}}c_{\mathbf{P},\mathbf{P}-\mathbf{k},\mathbf{q}}V_{\mathbf{q}}\right)\Bigg),\end{aligned}\tag{21}$$

$$\begin{aligned}\langle n_{\mathbf{k}\downarrow}\rangle\simeq&\frac{1}{2}-\frac{1}{2}\delta_{\mathbf{k},\mathbf{P}}(1-\delta\lambda)a^2_{\mathbf{P}}+\frac{1}{N}\Bigg(-(1-\delta\lambda)\sum_{\mathbf{q}}c^2_{\mathbf{P},\mathbf{q},\mathbf{P}-\mathbf{k}-\mathbf{q}}\\&-\sum_{\mathbf{q}}b^2_{\mathbf{P},\mathbf{P}-\mathbf{k}-\mathbf{q}}V^2_{\mathbf{q}}-\sum_{\mathbf{q}}b^2_{\mathbf{P},\mathbf{q}}\\&-2\sum_{\mathbf{q}}b_{\mathbf{P},\mathbf{P}-\mathbf{k}-\mathbf{q}}c_{\mathbf{P},\mathbf{P}-\mathbf{k}-\mathbf{q},\mathbf{q}}U_{\mathbf{q}}\Bigg).\end{aligned}$$

As we will show below, these expressions give good *quantitative* agreements with numerical data. As before, $\langle n_{\mathbf{k}\downarrow}\rangle$ shows a dip at $\mathbf{k}=\mathbf{P}$ with a weight proportional to the quasiparticle residue due to the center of the polaron. A constant positive (negative) shift due to different amount of spin excitations (fourth term) is also present in $\langle n_{\mathbf{k}\uparrow}\rangle$ ($\langle n_{\mathbf{k}\downarrow}\rangle$). The first three terms in $\langle n_{\mathbf{k}\uparrow}\rangle$ and the second and third terms in $\langle n_{\mathbf{k}\downarrow}\rangle$ reflect the hole distribution inside the polaron, whereas

the last two terms in $\langle n_{\mathbf{k}\uparrow}\rangle$ and the last term in $\langle n_{\mathbf{k}\downarrow}\rangle$ are from the interstring matrix elements. As before, they are odd with respect to the transformation $\mathbf{k}\to\mathbf{k}+\mathbf{Q}$ and lead to the formation of the dome structure in the EMDF. As we noted, the asymmetric term in $\langle n_{\mathbf{k}\downarrow}\rangle$ comes from the matrix element between the second and third components of the wave function of Eq. (20). We restrict ourselves to the first three components of Eq. (20) because for $J/t=0.3$ they give about 98% of the norm of the wave function. (We note that in the SCBA approach the same approximation gives about 92% of the norm[32]).

Formally, Eqs. (21) give a $1/N$ scaling for $\langle \delta n_{\mathbf{k}\sigma}\rangle$ at every $\mathbf{k}$ point except for the dip in $\langle \delta n_{\mathbf{k}\downarrow}\rangle$ at $\mathbf{k}=\mathbf{P}$. It fails at the point $\mathbf{k}=\mathbf{P}-\mathbf{Q}_{AF}$ where some of the terms in Eq. (21) are singular. The reason for these singularities is a peculiarity of the spin-polaron ground state and the AF long-range order. The dressing of the hole in the Néel background involves an infinite amount of zero-energy $\mathbf{q}=\mathbf{Q}$ spin excitations (whose total contribution to the hole weight is finite and small due to the diminishing magnon density of states). Since the EMDF probes the inner structure of the ground state it is actually measuring this singular probability of the virtual emission of a zero-energy magnon ($\mathbf{Q}$) by the hole ($\mathbf{P}$) if $\mathbf{k}$ is equal to $\mathbf{P}-\mathbf{Q}$.[83] This leads to singularities of different types for $\langle n_{\mathbf{k}\uparrow}\rangle$ and $\langle n_{\mathbf{k}\downarrow}\rangle$:

$$\langle n_{\mathbf{k}\uparrow}\rangle\sim\frac{1}{N}\frac{1}{\omega(\mathbf{k}-(\mathbf{P}-\mathbf{Q}))},\quad \langle n_{\mathbf{k}\downarrow}\rangle\sim\frac{1}{N}\ln\omega(\mathbf{k}-(\mathbf{P}-\mathbf{Q})), \tag{22}$$

where $\omega(\mathbf{k})$ is the magnon energy. For the finite system the magnon spectrum has the finite-energy gap at $\mathbf{Q}_{AF}$ which scales as[84,85]

$$\Delta E=J\frac{c^2}{\rho_s}\frac{1}{N}\left(1-\frac{c}{\rho_s}\frac{3.9}{4\pi}\frac{1}{\sqrt{N}}+\cdots\right), \tag{23}$$

where $c\simeq1.67$ and $\rho_s\simeq0.175$ (Ref. 86) are the spin-wave velocity and spin stiffness, respectively. This result gives antidips reported in Sec. III with the following scaling laws:

$$\langle n_\uparrow(\mathbf{P}-\mathbf{Q})\rangle\simeq\frac{1}{2}+\frac{C_\uparrow}{N}-B_{0\uparrow}-\frac{B_{1\uparrow}}{\sqrt{N}}+\frac{B_{2\uparrow}}{N},$$

$$\langle n_\downarrow(\mathbf{P}-\mathbf{Q})\rangle\simeq\frac{1}{2}-\frac{C_\downarrow}{N}-\frac{B_\downarrow\ln(C_0N)}{N}, \tag{24}$$

where all constants are positive. $C_\uparrow$, $C_\downarrow$ are from the ''regular'' part of Eq. (21). An interesting result shown in Eq. (24) is that the antidip in $\langle n_\uparrow(\mathbf{k})\rangle$ is predicted to survive in the thermodynamic limit:

$$\langle n_\uparrow(-\pi/2,-\pi/2)\rangle\sim Z_{\mathbf{P}}\rho_s/c^2\simeq0.07\cdot Z_{\mathbf{P}}, \tag{25}$$

whereas all other features except for the dip at $\mathbf{P}$ in $\langle n_\downarrow(\mathbf{k})\rangle\sim Z_{\mathbf{P}}$ will disappear. One can see from Eq. (24) that the scaling laws of the antidips are quite complicated. For a system as small as $N=32$, terms of different order in N have similar amplitudes. For example, $B_{1\uparrow}/\sqrt{32}\simeq0.5B_{0\uparrow}$. This makes the FSS for the antidips complicated, especially when only two of available clusters (16 and 32) possess this $\mathbf{k}$ point. An additional complication comes from the fact that the gap ΔE, Eq. (23), is calculated for the system without holes and the influence of the latter on it is not known. In the subsequent calculation of the EMDF for antidips we modify the magnon spectrum employed in Eq. (21) in a way that it has a gap ΔE at $\mathbf{q}=\mathbf{Q}$ point.[87]

The two-hole problem has been considered using the Hamiltonian of Eq. (17) in Ref. 19. A bound state with $d_{x^2-y^2}$ symmetry was found for $0<t/J<5$. The wave function of the d-wave bound state with total momentum $\mathbf{P}=0$ can be written in terms of creation operators of polarons of Eq. (20),

$$|2\rangle=|\Psi^d_{\mathbf{P}=0}\rangle=\sqrt{\frac{2}{N}}\sum_{\mathbf{p}}\Delta^d_{\mathbf{p}}\tilde{f}^\dagger_{\mathbf{p}}\tilde{g}^\dagger_{-\mathbf{p}}|0\rangle, \tag{26}$$

$$\begin{aligned}\Delta^d_{\mathbf{p}}&=\sum_{n=1}^{\infty}\sum_{m=-\infty}^{\infty}C_{2n-1,2m}\{\cos([2n-1]p_x+2mp_y)\\&\quad-\cos(2mp_x+[2n-1]p_y)\}\\&=C_{1,0}\{\cos(p_x)-\cos(p_y)\}+C_{3,0}\{\cos(3p_x)-\cos(3p_y)\}\\&\quad+C_{1,2}\{\cos(p_x\pm2p_y)-\cos(p_y\pm2p_x)\}+\cdots,\end{aligned}$$

$$C_{2n-1,2m}=C_{2n-1,-2m}$$

where $\Delta^d_{\mathbf{p}}$ is the solution of an analog of the Schrödinger equation for the two-body problem. The form of $\Delta^d_{\mathbf{p}}$ ensures the d-wave symmetry of the state and that the centers of the polarons are always on different sublattices, which in turn guarantees $S^z=0$. $\Delta^d_{\mathbf{p}}$ has a more general form than the simple ''nearest-neighbor d-wave'' in the simplified example of Eq. (11). It has higher harmonics, which have substantial weight for realistic t/J. In what follows we show that our comparison leads us to the conclusion that the large higher harmonics of $\Delta^d_{\mathbf{p}}$ play an important role in determining the behavior of $C(r)$ and $\langle n_{\mathbf{k}}\rangle$.

Note that for the representative value $J/t=0.3$ about 42% of the *polarons* in the bound state are located at the nearest-neighbor sites and less than 2% are farther than seven lattice spaces. An interesting feature of this distribution is that the probability in finding the second polaron at a certain distance from the first falls off slower along the x and y directions. Thus, the weight of the (3,0) $[\cos(3p_x)-\cos(3p_y)]$ harmonic of $\Delta^d_{\mathbf{p}}$ is rather large (20%), whereas the weight of (1,2) $[\cos(p_x\pm2p_y)-\cos(2p_x\pm p_y)]$ component is less than 5%.

Finally, relating the previous forms of the wave function (in terms of creation operators of holes and magnons) Eq. (26) becomes

$$\begin{aligned}|2\rangle&=\sqrt{\frac{2}{N}}\sum_{\mathbf{p}}\Delta^d_{\mathbf{p}}e^{\mathcal{S}}f^\dagger_{\mathbf{p}}g^\dagger_{-\mathbf{p}}|0\rangle\\&=\sqrt{\frac{2}{N}}\sum_{\mathbf{p}}\Delta^d_{\mathbf{p}}[\hat{\Delta}^\dagger_0(\mathbf{p})+\hat{\Delta}^\dagger_1(\mathbf{p})+\hat{\Delta}^\dagger_2(\mathbf{p})+]|0\rangle,\end{aligned}$$

$$\begin{aligned}\hat{\Delta}^\dagger_0(\mathbf{p})&=A^{(1)}_{\mathbf{p}}f^\dagger_{\mathbf{p}}g^\dagger_{-\mathbf{k}}+\sum_{\mathbf{q}}A^{(2)}_{\mathbf{p},\mathbf{q}}g^\dagger_{\mathbf{k}-\mathbf{q}}f^\dagger_{-\mathbf{k}+\mathbf{q}}\\&\quad+\sum_{\mathbf{q},\mathbf{q}'}A^{(3)}_{\mathbf{p},\mathbf{q},\mathbf{q}'}f^\dagger_{\mathbf{k}-\mathbf{q}-\mathbf{q}'}g^\dagger_{-\mathbf{k}+\mathbf{q}+\mathbf{q}'}+\cdots,\end{aligned} \tag{27}$$

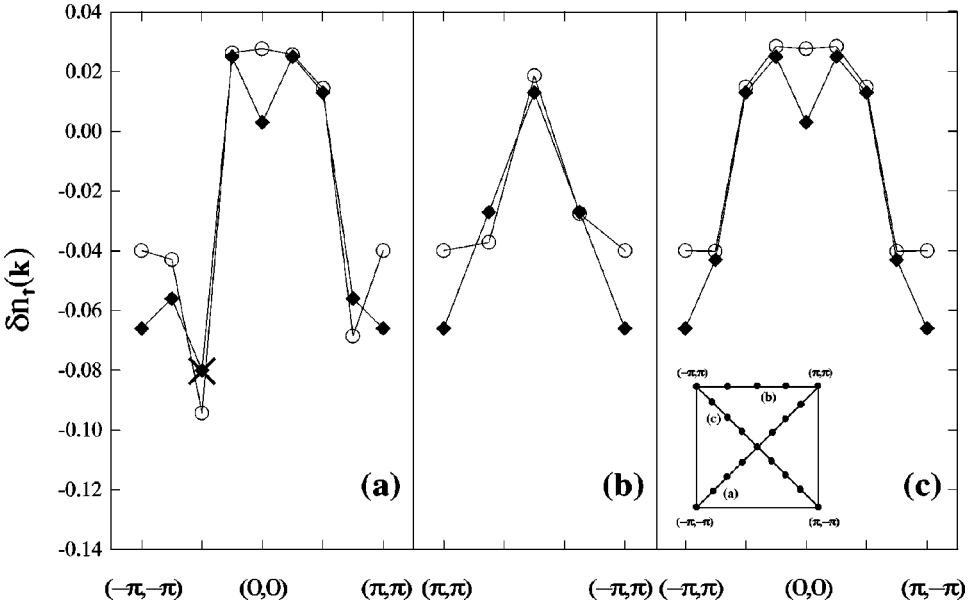

FIG. 11. Comparison of the numerical (open circles) and analytical (filled diamonds) results for $\langle \delta n_{\mathbf{k}\uparrow} \rangle$ in the single-hole ground state at $J/t=0.3$ along the lines shown in the inset $[(-\pi,-\pi) \rightarrow (\pi,\pi) \rightarrow (-\pi,\pi) \rightarrow (\pi,-\pi)]$. Solid lines are guides to the eye.

$$\hat{\Delta}_1^\dagger(\mathbf{p}) = \sum_{\mathbf{q}} \left[B^{(1)}_{\mathbf{p},\mathbf{q}} f^\dagger_{\mathbf{p}} f^\dagger_{-\mathbf{p}-\mathbf{q}} + \sum_{\mathbf{q}'} B^{(2)}_{\mathbf{p},\mathbf{q},\mathbf{q}'} f^\dagger_{\mathbf{p}-\mathbf{q}'-\mathbf{q}} f^\dagger_{-\mathbf{p}+\mathbf{q}'} + \cdots \right] \beta^\dagger_{\mathbf{q}} + \sum_{\mathbf{q}} \left[B^{(1)}_{-\mathbf{p},\mathbf{q}} g^\dagger_{\mathbf{p}-\mathbf{q}} g^\dagger_{-\mathbf{p}} + \sum_{\mathbf{q}'} B^{(2)}_{-\mathbf{p},\mathbf{q},\mathbf{q}'} g^\dagger_{\mathbf{p}+\mathbf{q}'} g^\dagger_{-\mathbf{p}-\mathbf{q}-\mathbf{q}'} + \cdots \right] \alpha^\dagger_{\mathbf{q}},$$

$$\hat{\Delta}_2^\dagger(\mathbf{p}) = \sum_{\mathbf{q},\mathbf{q}'} [C^{(1)}_{\mathbf{p},\mathbf{q},\mathbf{q}'} f^\dagger_{\mathbf{p}-\mathbf{q}-\mathbf{q}'} g^\dagger_{-\mathbf{p}} + C^{(1)}_{-\mathbf{p},\mathbf{q}',q} f^\dagger_{\mathbf{p}} g^\dagger_{-\mathbf{p}-\mathbf{q}-\mathbf{q}'} + C^{(2)}_{\mathbf{p},\mathbf{q},\mathbf{q}'} g^\dagger_{\mathbf{p}-\mathbf{q}} f^\dagger_{-\mathbf{p}-\mathbf{q}'} + \cdots] \alpha^\dagger_{\mathbf{q}} \beta^\dagger_{\mathbf{q}'},$$

where the subscripts n of $\hat{\Delta}$'s indicate the number of magnons in the corresponding component of the wave function.

Results of the EMDF and $C(r)$ in Eq. (19) for the ground state of Eq. (27) are given in full detail in the Appendix. In the next section we use these expressions to compare this theory with the numerical data discussed earlier in this paper.

V. COMPARISON OF NUMERICAL AND ANALYTICAL RESULTS

This section summarizes the comparison of our numerical ED data with the analytical results obtained from the CT approach. We focus on the EMDF for one and two holes, the binding energy, and the hole-hole correlation function for two holes. These provide a representative juxtaposition of results obtained from these two techniques, and probe in detail the correlations found in the ground states.

Figures 11–14 show our analytical results for the single-

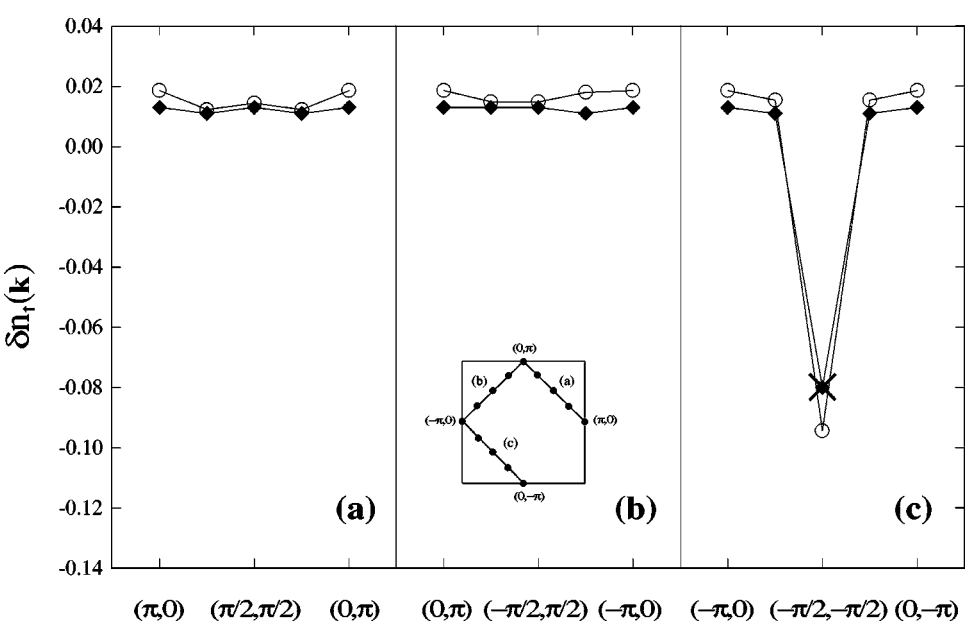

FIG. 12. The same as in Fig. 11 along the lines $[(\pi,0) \rightarrow (0,\pi) \rightarrow (-\pi,0) \rightarrow (0,-\pi)]$.

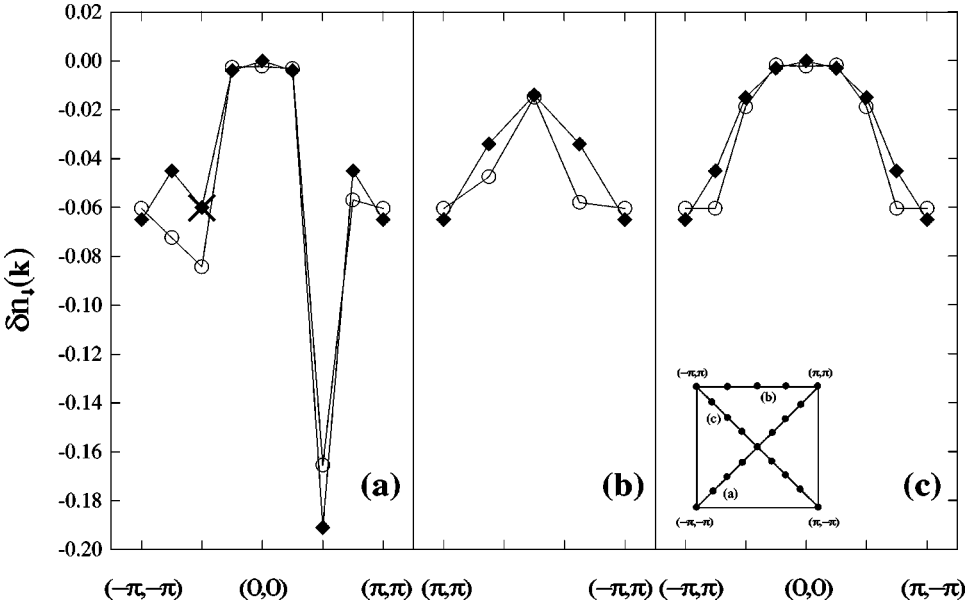

FIG. 13. Comparison of the numerical (open circles) and analytical (filled diamonds) results for $\langle \delta n_{\mathbf{k}\downarrow} \rangle$ in the single-hole ground state at $J/t=0.3$ along the lines shown in the inset $[(-\pi,-\pi) \rightarrow (\pi,\pi) \rightarrow (-\pi,\pi) \rightarrow (\pi,-\pi)]$. Solid lines are guides to the eye.

hole EMDF [Eq. (21)] together with the 32-site ED data. Solid lines are guides to the eye. The agreement is good for both spin directions. The differences between the $\langle \delta n_{\mathbf{k}\uparrow} \rangle$ numerical and analytical data at (0,0) and (π,π) can be attributed to the fact that the CT quasiparticle residue $Z_{\mathbf{k}}=a_{\mathbf{k}}^2$ at these points is larger than the ''exact'' values (e.g., SCBA). As one can see from Eq. (21), this leads to lower values of $\langle \delta n_{\mathbf{k}\uparrow} \rangle$. The agreement of the $\langle \delta n_{\mathbf{k}\downarrow} \rangle$ quantities away from $\mathbf{k}=\mathbf{P}$ is better because the role of the background does not depend on $a_{\mathbf{k}}$. The antidips in the analytical results are marked by the cross notifying that these points were calculated from Eq. (21) using a finite gap value in the magnon spectrum.[87]

As we discussed in Sec. IV, the internal structure of the spin polaron is made evident in the EMDF through the normal and interstring terms. The normal terms reflect the distribution of the hole inside of the spin-polaron wave function, viz. strings of different length. Interstring matrix elements are nonzero for $\langle \delta n_{\mathbf{k}} \rangle$ due to the specific structure of the spin polaron. They make a contribution to the EMDF Eqs.(10),(21), which is asymmetric under the transformation $\mathbf{k} \rightarrow \mathbf{k}+\mathbf{Q}$. These asymmetric terms are responsible for the dome shape of $\langle \delta n_{\mathbf{k},\sigma} \rangle$, as was proposed in Ref. 15, thus showing that it is not related to a Fermi surface signature.

The J/t dependence of the single-hole EMDF data has been extensively studied in Ref. 58 for smaller systems. As we already noted in Sec. IV, Eq. (21) naturally describes the results of these studies and of the observations made in Sec. III A. To be specific, the depth of the dip is proportional to $Z_{\mathbf{P}}$, and thus $\langle \delta n_{\mathbf{P},\downarrow} \rangle$ must follow the J/t dependence of $Z_{\mathbf{P}}$ (result of Ref. 58). Also, the background must be getting weaker for larger J/t because less hole weight is accumulated in the string cloud. The smaller values and stronger J/t dependence of $\Delta n_{\downarrow}$ and $\Delta n_{anti,\downarrow}$ are due to the second and third components of the spin-polaron wave function involved in the formation of the $\langle \delta n_{\mathbf{k},\downarrow} \rangle$ background, which are more sensitive to J/t.

Now we consider two-hole results, beginning with the

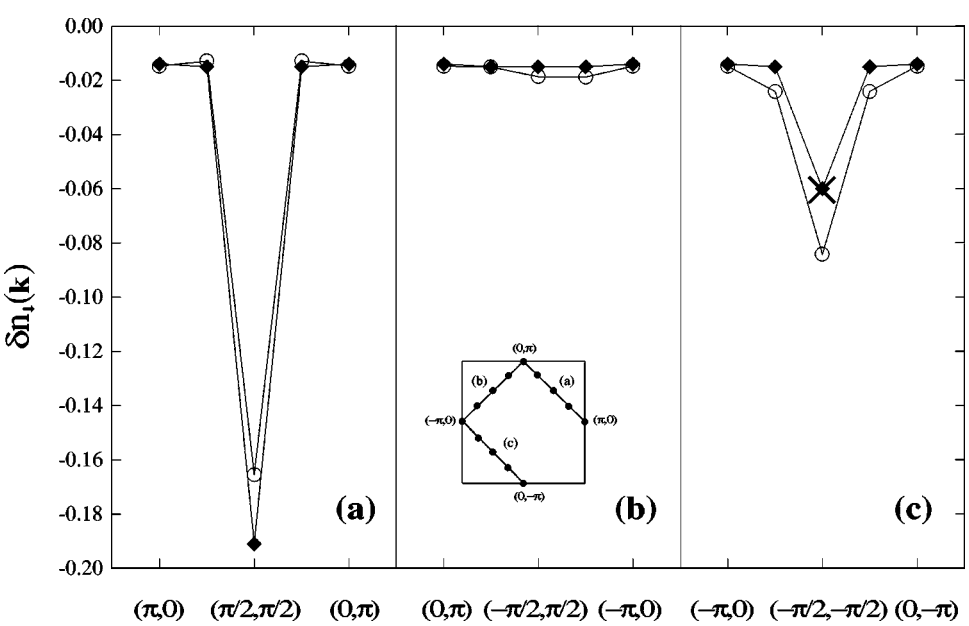

FIG. 14. The same as in Fig. 13 along the lines $[(\pi,0) \rightarrow (0,\pi) \rightarrow (-\pi,0) \rightarrow (0,-\pi)]$.

TABLE I. Amplitudes ($C_{2n-1,2m}$) and weights ($C^2_{2n-1,2m}$) of the harmonics in the spin-polaron bound-state wave function, Eq. (26). Weights are directly related to the polaron-polaron spatial distribution function: $P(r_{ll'})=(1/z_{ll'})C^2_{ll'}$, $z_{ll'}=4$; 8 is the coordination number. l and l' belong to different sublattices.

$(2n-1,2m)$	$C_{2n-1,2m}$	$C^2_{2n-1,2m}$, %
(1,0)	0.642	41.3
(1,2),(1,−2)	-0.108	4.6
(3,0)	-0.444	19.7
(3,2),(3,−2)	0.160	10.2
(5,0)	0.240	5.8

binding energy. This quantity for d-wave bound states was obtained numerically and analytically at a variety of J/t. For $J/t=0.3$ it was found that $E_b^{ED}=-0.05t$ and $E_b^{CT}=-0.02t$. As discussed before, the absence of a simple scaling law for E_b does not allow one to produce a reliable estimate of its thermodynamic limit at small J/t. Nevertheless, we believe that the close agreement of the energies supports the idea that the systems under study represent the same physics. A simple $1/N$ FSS for the larger $J/t=1.0$, where the size of the bound state is smaller and it is hoped that such a FSS will be more credible, gives a thermodynamic value of $E_b^{ED}\simeq-0.32t$ [Fig. 6(b)], which is very close to the theoretical result $E_b^{CT}=-0.38t$.

Figure 7(a) shows our results for the hole-hole correlation function $C(r)$ for two holes in the d-wave bound state, for $J/t=0.3$. This expectation value is calculated first for a bulk lattice, and then mapped onto the equivalent sites of a 32-site cluster with periodic boundary conditions. This enforces that the analytical work approximate some of the finite-size effects of our ED numerics, and facilitates a more natural comparison between the two. Very similar trends are found in both results, with the correlation function decreasing quite similarly with the distance.

Both numerical and analytical results data show that about 45% of the time the holes prefer to stay at the nearest- and next-nearest-neighbor distances. That our analytical work produces such behavior is not inconsistent with our statement regarding the form of $\Delta^d_{\mathbf{p}}$ Eq. (26): the *centers* of the polarons are indeed restricted to be on opposite sublattices, but the holes are almost equally distributed on both sublattices, with the maximum probability of separation being at $\sqrt{2}$. In fact, our analysis of the harmonics in $\Delta^d_{\mathbf{p}}$ given in Table I shows that about 40% of the *polarons* in the bound state are separated by one lattice constant. Thus, the peak of $C(r)$ at $r=\sqrt{2}$ arises from the components of the wave function with strings of length one. Clearly, the spin-polaron picture provides a natural explanation for the $\sqrt{2}$ paradox found here and in earlier numerical studies.

We believe that there are two reasons for the analytical $C(1)$ being slightly larger than $C(\sqrt{2})$. A treatment of the t-J model based on the spinless hole representation involves some unphysical states with the hole and spin excitations being at the same site. The number of processes leading to such states increases when the polarons are close to each other and hence $C(1)$ grows. Secondly, the CT approach slightly overestimates bare hole weight.

An additional maximum in our analytical $C(r)$ at $r=3$ is closely connected to the second important harmonic in the CT $d_{x^2-y^2}$ bound state $\sim[\cos(3p_x)-\cos(3p_y)]$. We cannot explain the absence of such a peak in the ED results—for example, we have been unable to estimate the finite-size effect on individual harmonics in the two-hole wave function.

Figure 7(b) demonstrates a better agreement at $J/t=0.8$ when the size of the bound state is small. In this case the correlation falls rapidly with distance and thus the ''bulk to cluster'' mapping does not alter the analytical data. Therefore, in the large J/t limit we find the expected result that a spin-polaron approach adequately describes the physics.

The EMDF for two holes shows an equally satisfactory comparison, as seen in Fig. 15. The behavior of $\langle\delta n_{\mathbf{k}}\rangle$ involves the combined effects of (i) the internal structure of the polarons, (ii) the d-wave symmetry bound state, and (iii) higher harmonics in the bound-state wave function. We now elaborate on these features.

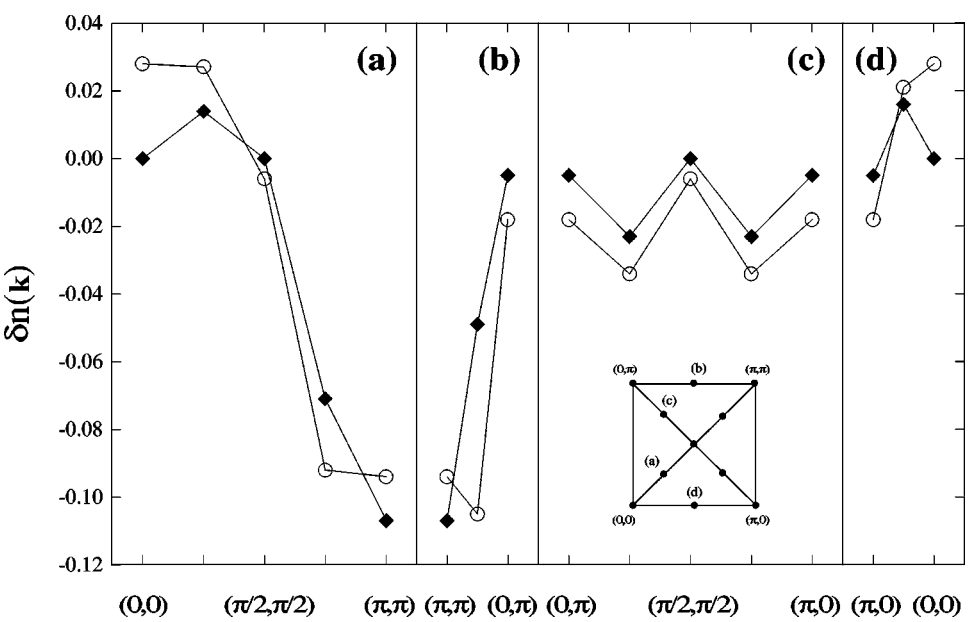

FIG. 15. Comparison of the numerical (open circles) and analytical (filled diamonds) results for $\langle\delta n_{\mathbf{k}\downarrow}\rangle$ in the two-hole ground state at $J/t=0.3$ along the lines shown in the inset $[(0,0)\rightarrow(\pi,\pi)\rightarrow(0,\pi)\rightarrow(\pi,0)\rightarrow(0,0)]$. Solid lines are guides to the eye.

As we argued in Sec. III B, the quantity $\Delta n^{2hole} = (\langle n_{(0,0)}\rangle - \langle n_{(\pi,\pi)}\rangle) \simeq (\Delta n_{\uparrow}^{1hole} + \Delta n_{\downarrow}^{1hole})$ shows that the overall background deviation is mainly irrelevant to the bound-state **k** structure. The worst agreement between ED and CT analytics for the (0,0) and (π,π) points (Fig. 15) is again due to the $Z_{\mathbf{k}=0}$ problem within the CT approach.

Next we focus on the features along the ABZ boundary which, as we discussed before, are not disguised by kinematic effects (all asymmetric and most of the normal terms are zero on this line) and can be directly related to the form of $\Delta_{\mathbf{p}}^{d}$ in Eq. (26). Our analytical and numerical $\langle \delta n_{\mathbf{k}}\rangle$ results have a local maximum at $\mathbf{k}=(\pi/2,\pi/2)$, and have minima at $(3\pi/4,\pi/4)$ and $(\pi/4,3\pi/4)$. The first feature can be explained by the *d*-wave symmetry of the bound state. The EMDF is reduced from its half-filled value of 1/2 when holes occupy that momentum state. However, as shown in Eq. (12), the EMDF consists of terms proportional to $(\Delta_{\mathbf{k}}^{d})^2$, which is identically zero at $(\pi/2,\pi/2)$. Thus, $\langle \delta n_{\mathbf{k}}\rangle$ must show a local maximum $(=0)$ at this wave vector, so one cannot find any direct remnant of hole pockets for $d_{x^2-y^2}$-wave symmetry bound state.

A second feature that we observe in both analytical and numerical results, viz. the minimum along the ABZ boundary between $(\pi,0)$ and $(\pi/2,\pi/2)$, can be related to the particular form of $\Delta_{\mathbf{p}}^{d}$. Analytically, this quantity has large and apparently important higher harmonics [see Table I and Eq. (26)], and it is the competition between the different harmonics that produces the maximum hole number between $(\pi/2,\pi/2)$ and $(3\pi/4,\pi/4)$. Our analytical work shows that the hole number is actually maximized along the ABZ boundary very close to $(\pi/2,\pi/2)$, roughly at $(0.45\pi,0.55\pi)$. It is unclear if experiments could resolve this feature.

VI. CONCLUSIONS

Summarizing, we have presented new ED numerical data for up to two holes in the *t*-*J* model for the largest cluster for which such calculations can be completed presently. Then, we compared these results with new analytical expressions based on the canonical transformation approach to the *t*-*J* model. We find good agreement for the binding energy, the EMDF for one and two holes, and the hole-hole spatial correlation function. We consider this to lend strong support to the validity of the quasiparticle Hamiltonian derived in Ref. 19, thus supporting the contention that the spin-polaron description of the quasiparticles in the *t*-*J* model is correct at least at low hole concentration.

Certain characteristics in the correlation functions we studied are direct consequences of some features of the corresponding ground state wave functions. For example, the dip in the single-hole spin $\downarrow$ EMDF is related to the center of the spin polaron, whereas the dome structure of the one- and two-hole EMDF is due to the interstring matrix elements of $\langle n_{\mathbf{k}\sigma}\rangle$. The large correlation between the holes in the *d*-wave bound state at a distance of $\sqrt{2}$ is due to the significant weight of the shortest string in the spin-polaron wave function. Analytical results for the FSS of the EMDF show a $1/N$ scaling at almost all **k** points except at the single-hole ground state **P** [Eqs. (10),(12),(21)], in agreement with what is shown in Sec. III for the ED data. Those **k** points that are influenced by the long-range physics of the system are shown to have more complicated scaling laws—see Eqs. (22),(24). The role of the higher harmonics and the effect of the size of the bound state on the EMDF and the hole-hole correlation function for the two-hole problem are also discussed.

ACKNOWLEDGMENTS

We would like to thank Martin Letz, Frank Marsiglio, T.-K. Ng, and Oleg Sushkov for helpful comments. We are grateful to R. Eder for correspondence and for supplying us with useful references. This work was supported by the RGC of Hong Kong, and the NSERC of Canada. The 32-site ED work was completed on the Intel Paragon at HKUST.

APPENDIX A: EMDF AND $C(r)$ FOR TWO-HOLE CASE

The amplitudes of the components of the two-hole wave function Eq. (27), $A^{(n)},B^{(n)},C^{(n)}$, can be expressed through the a,b,c components of the single-hole wave function of Eq. (20):

$$A_{\mathbf{k}}^{(1)}=a_{\mathbf{k}}^{2},\quad A_{\mathbf{k},\mathbf{q}}^{(2)}=2b_{\mathbf{k},\mathbf{q}}b_{-\mathrm{k}+\mathbf{q},\mathbf{q}},$$

$$A_{\mathbf{k},\mathbf{q},\mathbf{q}'}^{(3)}=c_{\mathbf{k},\mathbf{q},\mathbf{q}'}c_{-\mathbf{k}+\mathbf{q}+\mathbf{q}',\mathbf{q}',\mathbf{q}},$$

$$B_{\mathbf{k},\mathbf{q}}^{(1)}=-a_{\mathbf{k}}b_{-\mathbf{k},\mathbf{q}},\quad B_{\mathbf{k},\mathbf{q},\mathbf{q}'}^{(2)}=b_{\mathbf{k},\mathbf{q}'}b_{\mathbf{k}-\mathbf{q}',\mathbf{q}}b_{-\mathbf{k}+\mathbf{q}',\mathbf{q}'},\tag{A1}$$

$$C_{\mathbf{k},\mathbf{q},\mathbf{q}'}^{(1)}=\frac{1}{2}a_{\mathbf{k}}c_{\mathbf{k},\mathbf{q},\mathbf{q}'},\quad C_{\mathbf{k},\mathbf{q},\mathbf{q}'}^{(2)}=b_{\mathbf{k},\mathbf{q}}b_{-\mathbf{k},\mathbf{q}'}.$$

The quantities $a_{\mathbf{k}},b_{\mathbf{k},\mathbf{q}}$, and $c_{\mathbf{k},\mathbf{q},\mathbf{q}'}$, within the CT approach, are the products of $M_{\mathbf{k},\mathbf{q}}$'s of Eq. (14), the transformation parameter $f_{\mathbf{k}}$ of Eq. (16), and different integrals of their combinations given by

$$a_{\mathbf{k}}=\left[1-\frac{1}{2!}I_{\mathbf{k}}+\frac{1}{4!}(I_{\mathbf{k}}^{2}+F_{\mathbf{k}}^{(1)})-\frac{1}{6!}(I_{\mathbf{k}}^{3}+2I_{\mathbf{k}}F_{\mathbf{k}}^{(1)}+F_{\mathbf{k}}^{(2)}+F_{\mathbf{k}}^{(3)})\right],$$

$$b_{\mathbf{k},\mathbf{q}}=\mu_{\mathbf{k},\mathbf{q}}\left[1-\frac{1}{3!}(I_{\mathbf{k}}+I_{\mathbf{k}-\mathbf{q}})+\frac{1}{5!}(I_{\mathbf{k}}^{2}+F_{\mathbf{k}}^{(1)}+I_{\mathbf{k}}I_{\mathbf{k}-\mathbf{q}}+I_{\mathbf{k}-\mathbf{q}}^{2}+F_{\mathbf{k}-\mathbf{q}}^{(1)})\right],\tag{A2}$$

$$c_{\mathbf{k},\mathbf{q},\mathbf{q}'}=\mu_{\mathbf{k},\mathbf{q}}\mu_{\mathbf{k}-\mathbf{q},\mathbf{q}'}\left[\frac{1}{2!}-\frac{1}{4!}(I_{\mathbf{k}}+I_{\mathbf{k}-\mathbf{q}}+I_{\mathbf{k}-\mathbf{q}-\mathbf{q}'})+\frac{1}{6!}(I_{\mathbf{k}}I_{\mathbf{k}-\mathbf{q}}+I_{\mathbf{k}-\mathbf{q}}^{2}+I_{\mathbf{k}}I_{\mathbf{k}-\mathbf{q}-\mathbf{q}'}+I_{\mathbf{k}-\mathbf{q}}I_{\mathbf{k}-\mathbf{q}-\mathbf{q}'}+I_{\mathbf{k}-\mathbf{q}-\mathbf{q}'}^{2}+F_{\mathbf{k}-\mathbf{q}}^{(1)}+F_{\mathbf{k}-\mathbf{q}-\mathbf{q}'}^{(1)})\right],$$

$$\text{with}\quad I_{\mathbf{k}}=\sum_{\mathbf{q}}\mu^2_{\mathbf{k},\mathbf{q}},\quad F^{(1)}_{\mathbf{k}}=\sum_{\mathbf{q}}\mu^2_{\mathbf{k},\mathbf{q}}I_{\mathbf{k}-\mathbf{q}},$$

$$F^{(2)}_{\mathbf{k}}=\sum_{\mathbf{q}}\mu^2_{\mathbf{k},\mathbf{q}}F^{(1)}_{\mathbf{k}-\mathbf{q}},\quad F^{(3)}_{\mathbf{k}}=\sum_{\mathbf{q}}\mu^2_{\mathbf{k},\mathbf{q}}I^2_{\mathbf{k}-\mathbf{q}},$$

where $\mu_{\mathbf{k},\mathbf{q}}=f_{\mathbf{k}}M_{\mathbf{k},\mathbf{q}}$.

Using Eq. (19) and the bound-state wave function of Eq. (27) one can obtain the EMDF for the two-hole ground state,

$$\langle n_{\mathbf{k}}\rangle\simeq\frac{1}{2}+\frac{1}{N}[-\langle\delta n^{even}_{\mathbf{k}}\rangle+2\langle\delta n^{odd}_{\mathbf{k}}\rangle],$$

$$\langle\delta n^{even}_{\mathbf{k}}\rangle=FA^2_{\mathbf{k}}+\sum_{\mathbf{q}}FB^2_{\mathbf{k},\mathbf{q}}+\sum_{\mathbf{q},\mathbf{q}'}FC^2_{\mathbf{k},\mathbf{q},\mathbf{q}'},\tag{A3}$$

$$\langle\delta n^{odd}_{\mathbf{k}}\rangle=\sum_{\mathbf{q}}FB_{\mathbf{k},\mathbf{q}}U_{\mathbf{q}}FA_{\mathbf{k}+\mathbf{q}}-FA_{\mathbf{k}}\sum_{\mathbf{q}}V_{\mathbf{q}}FB_{\mathbf{k},\mathbf{q}}-\sum_{\mathbf{q},\mathbf{q}'}FC_{\mathbf{k},\mathbf{q},\mathbf{q}'}U_{\mathbf{q}'}FB_{\mathbf{k}+\mathbf{q}+\mathbf{q}',-q}+\sum_{\mathbf{q}'}FB_{\mathbf{k},\mathbf{q}'}\sum_{\mathbf{q}}V_{\mathbf{q}}FC_{\mathbf{k}+\mathbf{q}',-q,-q'},$$

where

$$FA_{\mathbf{k}}=\Delta^d_{\mathbf{k}}A^{(1)}_{\mathbf{k}}+\sum_{\mathbf{q}}\Delta^d_{\mathbf{k}+\mathbf{q}}A^{(2)}_{\mathbf{k}+\mathbf{q},\mathbf{q}}+\sum_{\mathbf{q},\mathbf{q}'}\Delta^d_{\mathbf{k}+\mathbf{q}+\mathbf{q}'}A^{(3)}_{\mathbf{k}+\mathbf{q}+\mathbf{q}',\mathbf{q},\mathbf{q}'},$$

$$FB_{\mathbf{k},\mathbf{q}}=\Delta^d_{\mathbf{k}}B^{(1)}_{\mathbf{k},\mathbf{q}}-\Delta^d_{\mathbf{k}+\mathbf{q}}B^{(1)}_{\mathbf{k}+\mathbf{q},-\mathbf{q}}+\sum_{\mathbf{q}'}(\Delta^d_{\mathbf{k}+\mathbf{q}+\mathbf{q}'}B^{(2)}_{\mathbf{k}+\mathbf{q}+\mathbf{q}',\mathbf{q},\mathbf{q}'}-\Delta^d_{\mathbf{k}+\mathbf{q}'}B^{(2)}_{\mathbf{k}+\mathbf{q}',-\mathbf{q},\mathbf{q}'},\tag{A4}$$

$$FC_{\mathbf{k},\mathbf{q},\mathbf{q}'}=\Delta^d_{\mathbf{k}+\mathbf{q}+\mathbf{q}'}C^{(1)}_{\mathbf{k}+\mathbf{q}+\mathbf{q}',\mathbf{q},\mathbf{q}'}+\Delta^d_{\mathbf{k}}C^{(1)}_{-\mathbf{k},\mathbf{q}',q}-\Delta^d_{\mathbf{k}+\mathbf{q}'}C^{(2)}_{\mathbf{k}+\mathbf{q}',-\mathbf{q},-\mathbf{q}'}.$$

The hole-hole correlation function of Eq. (19) in the bound state described in Eq. (27) is given by

$$C(r_{ij})\simeq\begin{cases}C^{00}(r_{ij})+C^{22}(r_{ij})=\langle 2|n^f_i n^g_j|2\rangle, & \text{when } i+j=2n-1\\ C^{11}(r_{ij})=\langle 2|n^f_i n^f_j|2\rangle, & \text{when } i+j=2n\end{cases}$$

$$C^{00}(r_{ij})=\left[\sum_{\mathbf{k}}\Delta^d_{\mathbf{k}}\left(A^{(1)}_{\mathbf{k}}\cos[\mathbf{k}\mathbf{r}_{ij}]+\sum_{\mathbf{q}}A^{(2)}_{\mathbf{k},\mathbf{q}}\cos[(\mathbf{k}-\mathbf{q})\mathbf{r}_{ij}]+\sum_{\mathbf{q},\mathbf{q}'}A^{(3)}_{\mathbf{k},\mathbf{q},\mathbf{q}'}\cos[(\mathbf{k}-\mathbf{q}-\mathbf{q}')\mathbf{r}_{ij}]\right)\right]^2,\tag{A5}$$

$$C^{11}(r_{ij})=\sum_{\mathbf{k},\mathbf{p}}\Delta^d_{\mathbf{k}}\Delta^d_{\mathbf{p}}\sum_{\mathbf{q}}\left(B^{(1)}_{\mathbf{k},\mathbf{q}}B^{(1)}_{\mathbf{p},\mathbf{q}}\{\cos[(\mathbf{k}-\mathbf{p})\mathbf{r}_{ij}]-\cos[(\mathbf{k}+\mathbf{p}+\mathbf{q})\mathbf{r}_{ij}]\}+2B^{(1)}_{\mathbf{k},\mathbf{q}}\sum_{\mathbf{q}'}B^{(2)}_{\mathbf{k},\mathbf{q},\mathbf{q}'}\{\cos[(\mathbf{k}-\mathbf{p}+\mathbf{q}+\mathbf{q}')\mathbf{r}_{ij}]-\cos[(\mathbf{k}+\mathbf{p}-\mathbf{q}')\mathbf{r}_{ij}]\}\right),$$

$$C^{22}(r_{ij})=\sum_{\mathbf{k},\mathbf{p}}\Delta^d_{\mathbf{k}}\Delta^d_{\mathbf{p}}\sum_{\mathbf{q},\mathbf{q}'}\{(C^{(1)}_{\mathbf{k},\mathbf{q},\mathbf{q}'}C^{(1)}_{\mathbf{p},\mathbf{q},\mathbf{q}'}+C^{(1)}_{-\mathbf{k},\mathbf{q}',\mathbf{q}}C^{(1)}_{-\mathbf{p},\mathbf{q}',\mathbf{q}}+C^{(2)}_{\mathbf{k},\mathbf{q},\mathbf{q}'}C^{(2)}_{\mathbf{p},\mathbf{q},\mathbf{q}'})\cos[(\mathbf{k}-\mathbf{p})\mathbf{r}_{ij}]+2C^{(1)}_{\mathbf{k},\mathbf{q}',\mathbf{q}}C^{(1)}_{-\mathbf{p},\mathbf{q}',\mathbf{q}}\cos[(\mathbf{k}-\mathbf{p}+\mathbf{q}+\mathbf{q}')\mathbf{r}_{ij}]-2C^{(2)}_{\mathbf{k},\mathbf{q}',\mathbf{q}}C^{(1)}_{\mathbf{p},\mathbf{q},\mathbf{q}'}\cos[(\mathbf{k}+\mathbf{p}-\mathbf{q}')\mathbf{r}_{ij}]-2C^{(2)}_{\mathbf{k},\mathbf{q},\mathbf{q}'}C^{(1)}_{-\mathbf{p},\mathbf{q}',\mathbf{q}}\cos[(\mathbf{k}+\mathbf{p}+\mathbf{q}')\mathbf{r}_{ij}]\}.$$

*On leave from the Institute of Semiconductor Physics, Novosibirsk, 630090, Russia.

[1] P. W. Anderson, Science **235**, 1196 (1987).
[2] For a recent review, see E. Dagotto, Rev. Mod. Phys. **66**, 763 (1994).
[3] F. C. Zhang and T. M. Rice, Phys. Rev. B **37**, 3759 (1988).
[4] B. O. Wells *et al.*, Phys. Rev. Lett. **74**, 964 (1995).
[5] P. W. Leung, B. O. Wells, and R. J. Gooding, Phys. Rev. B **56**, 6320 (1997).
[6] A. Nazarenko, K. J. E. Vos, S. Haas, E. Dagotto, and R. J. Gooding, Phys. Rev. B **51**, R8676 (1995).
[7] V. I. Belinicher, A. L. Chernyshev, and V. A. Shubin, Phys. Rev. B **54**, 14 914 (1996).
[8] K. J. E. Vos and R. J. Gooding, Z. Phys. B **101**, 79 (1996).
[9] P. W. Anderson, Adv. Phys. **46**, 3 (1997).
[10] P. W. Leung and R. J. Gooding, Phys. Rev. B **52**, R15 711 (1995); **54**, 711 (1996); in *Proceedings of the 10th Anniversary of the HTS Workshop on Physics, Materials and Applications,*

edited by B. Batlogg *et al.* (World Scientific, Singapore, 1996), p. 525.
[11] L. N. Bulaevskii, E. L. Nagaev, and D. I. Khomskii, Zh. Éksp. Teor. Fiz. **54**, 1562 (1968) [Sov. Phys. JETP **27**, 638 (1967)].
[12] C. L. Kane, P. A. Lee, and N. Read, Phys. Rev. B **39**, 6880 (1989).
[13] Z. Liu and E. Manousakis, Phys. Rev. B **45**, 2425 (1992); **51**, 3156 (1995).
[14] G. Martínez and P. Horsch, Phys. Rev. B **44**, 317 (1991).
[15] R. Eder and K. W. Becker, Phys. Rev. B **44**, 6982 (1991).
[16] R. Eder and P. Wróbel, Phys. Rev. B **47**, 6010 (1993).
[17] R. Eder, Phys. Rev. B **45**, 319 (1992); P. Wróbel and R. Eder, *ibid.* **49**, 1233 (1994).
[18] J. A. Riera and E. Dagotto, Phys. Rev. B **55**, 14 543 (1997).
[19] V. I. Belinicher, A. L. Chernyshev, and V. A. Shubin, Phys. Rev. B **56**, 3381 (1997); the extended version of the paper (Report No. cond-mat/9611001).
[20] W. F. Brinkman and T. M. Rice, Phys. Rev. B **2**, 1324 (1970).
[21] S. Schmitt-Rink, C. M. Varma, and A. E. Ruckenstein, Phys. Rev. Lett. **60**, 2793 (1988).
[22] F. Marsiglio, A. E. Ruckenstein, S. Schmitt-Rink, and C. M. Varma, Phys. Rev. B **43**, 10 882 (1991).
[23] S. Trugman, Phys. Rev. B **37**, 1597 (1988); **41**, 892 (1990).
[24] G. Reiter, Phys. Rev. B **49**, 1536 (1994).
[25] R. Eder and K. W. Becker, Z. Phys. B **78**, 219 (1990); **79**, 333 (1990); R. Eder, K. W. Becker, and W. H. Stephan, **81**, 33 (1990).
[26] E. Dagotto and J. R. Schrieffer, Phys. Rev. B **43**, 8705 (1991).
[27] O. P. Sushkov, Solid State Commun. **83**, 303 (1992).
[28] A. V. Dotsenko, Phys. Rev. B **57**, 6917 (1998).
[29] J. Bala, A. M. Oleś, and J. Zaanen, Phys. Rev. B **52**, 4597 (1995).
[30] B. Shraiman and E. Siggia, Phys. Rev. Lett. **61**, 467 (1988); Phys. Rev. B **42**, 2485 (1990).
[31] O. A. Starykh and G. Reiter, Phys. Rev. B **53**, 2517 (1996).
[32] A. Ramsak and P. Horsch, Phys. Rev. B **48**, 10 559 (1993).
[33] N. M. Plakida, P. Horsch, A. Liechtenstein, and V. S. Oudovenko, Phys. Rev. B **55**, 11 997 (1997).
[34] R. Eder and Y. Ohta, Phys. Rev. B **50**, 10 043 (1994).
[35] B. Shraiman and E. Siggia, Phys. Rev. Lett. **60**, 740 (1988).
[36] M. Kuchiev and O. Sushkov, Physica C **218**, 197 (1993).
[37] J. R. Schrieffer, X.-G. Wen, and S.-C. Zhang, Phys. Rev. Lett. **60**, 944 (1988); A. Kampf and J. R. Schrieffer, Phys. Rev. B **41**, 6399 (1990); J. R. Schrieffer, X. G. Wen, and S. C. Zhang, *ibid.* **39**, 11 663 (1989).
[38] V. Flambaum, M. Kuchiev, and O. Sushkov, Physica C **227**, 267 (1994); V. I. Belinicher, A. L. Chernyshev, A. V. Dotsenko, and O. P. Sushkov, Phys. Rev. B **51**, 6076 (1995).
[39] E. Dagotto, A. Nazarenko, and A. Moreo, Phys. Rev. Lett. **74**, 310 (1995); A. Nazarenko, A. Moreo, E. Dagotto, and J. Riera, Phys. Rev. B **54**, 768 (1996).
[40] B. Shraiman and E. Siggia, Phys. Rev. B **40**, 9162 (1989).
[41] A. Cherhyshev, A. Dotsenko, and O. Sushkov, Phys. Rev. B **49**, 6197 (1994).
[42] O. Sushkov, Phys. Rev. B **49**, 1250 (1994).
[43] D. Frenkel and W. Hanke, Phys. Rev. B **42**, 6711 (1990).
[44] J. Bonča, P. Prelovšek, and I. Sega, Phys. Rev. B **39**, 7074 (1989).
[45] D. Poilblanc and E. Dagotto, Phys. Rev. B **42**, 4861 (1990).
[46] J. A. Riera and A. P. Young, Phys. Rev. B **39**, 9697 (1989).
[47] Y. Hasegawa and D. Poilblanc, Phys. Rev. B **40**, 9035 (1989).
[48] E. Dagotto, A. Moreo, R. Joynt, S. Bacci, and E. Gagliano, Phys. Rev. B **41**, 2585 (1990); **41**, 9049 (1990); E. Gagliano, S. Bacci, and E. Dagotto, *ibid.* **42**, 6222 (1990).
[49] E. Dagotto, J. A. Riera, and A. P. Young, Phys. Rev. B **42**, 2347 (1990).
[50] J. A. Riera, Phys. Rev. B **43**, 3681 (1991).
[51] H.-Q. Ding, Physica C **203**, 91 (1992).
[52] T. Barnes, A. E. Jacobs, M. D. Kovarik, and W. G. Macready, Phys. Rev. B **45**, 256 (1992).
[53] V. Elser, D. A. Huse, B. Shraiman, and E. Siggia, Phys. Rev. B **41**, 6715 (1990).
[54] K. J. von Szczerpanski, P. Horsch, W. Stephan, and M. Ziegler, Phys. Rev. B **41**, 2017 (1990).
[55] T. Itoh, M. Arai, and T. Fujiwara, Phys. Rev. B **42**, 4834 (1990).
[56] H. Fehske, V. Waas, H. Röder, and H. Büttner, Phys. Rev. B **44**, 8473 (1991).
[57] W. Stephan and P. Horsch, Phys. Rev. Lett. **66**, 2258 (1991).
[58] R. Eder and Y. Ohta, Phys. Rev. B **51**, 6041 (1995).
[59] R. Eder, Y. Ohta, and T. Shimozato, Phys. Rev. B **50**, 3350 (1994); S. Nishimoto, R. Eder, and Y. Ohta, Physica C **282-287**, 1731 (1997).
[60] Y. Ohta, T. Shimozato, and R. Eder, Phys. Rev. Lett. **73**, 324 (1994).
[61] R. Eder, Y. Ohta, and G. Sawatzky, Phys. Rev. B **55**, 3414 (1997).
[62] R. Eder, Y. Ohta, and S. Maekawa, Phys. Rev. Lett. **74**, 5124 (1995).
[63] D. Poilblanc, H. J. Schulz, and T. Ziman, Phys. Rev. B **46**, 6435 (1992).
[64] D. Poilblanc, H. J. Schulz, and T. Ziman, Phys. Rev. B **47**, 3268 (1993).
[65] D. Poilblanc, T. Ziman, H. J. Schulz, and E. Dagotto, Phys. Rev. B **47**, 14 267 (1992).
[66] P. Prelovšek, I. Sega, and J. Bonča, Phys. Rev. B **42**, 10 706 (1990).
[67] D. Poilblanc, Phys. Rev. B **48**, 3368 (1993).
[68] D. Poilblanc, Phys. Rev. B **49**, 1477 (1994).
[69] D. Poilblanc, J. Riera, and E. Dagotto, Phys. Rev. B **49**, 12 318 (1994).
[70] R. J. Gooding, K. J. E. Vos, and P. W. Leung, Phys. Rev. B **49**, 4119 (1994).
[71] K. J. E. Vos, R. J. Gooding, P. W. Leung, and L. Chen, Phys. Rev. B **51**, 12 034 (1995).
[72] P. Prelovšek and X. Zotos, Phys. Rev. B **47**, 5984 (1993).
[73] E. Kaxiras and E. Manousakis, Phys. Rev. B **38**, 866 (1988).
[74] J. A. Riera, Phys. Rev. B **40**, 833 (1989).
[75] M. Boninsegni and E. Manousakis, Phys. Rev. B **47**, 11 897 (1993).
[76] D. J. Scalapino, E. Loh, and J. E. Hirsch, Phys. Rev. B **35**, 6694 (1987).
[77] A. L. Chernyshev, P. W. Leung, and R. J. Gooding, Phys. Chem. Solids (to be published November 1998).
[78] S. R. White and D. J. Scalapino, Phys. Rev. B **55**, 6504 (1997).
[79] J. A. Riera and E. Dagotto, Phys. Rev. B **57**, 8609 (1998).
[80] O. Sushkov, G. Sawatzky, R. Eder, and H. Eskes, Phys. Rev. B **56**, 11 769 (1997).
[81] F. P. Onufrieva, V. P. Kushnir, and B. P. Toperverg, Phys. Rev. B **50**, 12 935 (1994).
[82] L. Yu, Z. B. Su, and Y. M. Li, Chin. J. Phys. **31**, 579 (1993).
[83] The second term in $\langle n_{\mathbf{k},\uparrow}\rangle$ $(\sim a_{\mathbf{P}}^2 V_{\mathbf{P}-\mathbf{k}}^2)$ reflects the response of the spin system to the insertion of a hole into the fluctuating spin

background. It also diverges at the $\mathbf{k}=\mathbf{P}-\mathbf{Q}_{AF}$ point.
[84] H. Neuberger and T. Ziman, Phys. Rev. B **39**, 2608 (1989).
[85] P. Hasenfratz and F. Niedermayer, Z. Phys. B **92**, 91 (1993).
[86] A. W. Sandvik, Phys. Rev. B **56**, 11 678 (1997).
[87] The value of the gap can be calculated from Eq. (23). The result in leading order in $1/N$ is $\Delta E=0.498J$. Taking into account the $1/\sqrt{N}$ correction change this result to $\Delta E=0.237J$. In the calculations we used the ED value of the gap, $\Delta E^{ED}=0.315J$. We believe that the use of this latter relation provides a reliable estimation of the EMDF quantities.